

Article

Testing Predictions of the Quantum Landscape Multiverse 3: The Hilltop Inflationary Potential

Eleonora Di Valentino ^{1,*}  and Laura Mersini-Houghton ²

¹ Jodrell Bank Center for Astrophysics, School of Physics and Astronomy, University of Manchester, Oxford Road, Manchester M13 9PL, UK

² Department of Physics and Astronomy, UNC-Chapel Hill, Chapel Hill, NC 27599, USA; mersini@physics.unc.edu

* Correspondence: eleonora.divalentino@manchester.ac.uk

Received: 14 March 2019; Accepted: 1 April 2019; Published: 10 April 2019



Abstract: Here we test the predictions of the theory of the origin of the universe from the landscape multiverse, against the 2015 Planck data, for the case of the Hilltop class of inflationary models, for $p = 4$ and $p = 6$. By considering the quantum entanglement correction of the multiverse, we can place just a lower limit on the local ‘SUSY-breaking’ scale, respectively $b > 8.7 \times 10^6 GeV$ at 95% c.l. and $b > 1.3 \times 10^8 GeV$ at 95% c.l. from Planck TT+lowP, so the case with multiverse correction is statistically indistinguishable from the case with an unmodified inflation. We find that the series of anomalies predicted by the quantum landscape multiverse for the allowed range of b , is consistent with Planck’s tests of the anomalies. In addition, the friction between the two cosmological probes of the Hubble parameter and with the weak lensing experiments goes away for a particular subset, the $p = 6$ case of Hilltop models.

Keywords: Cosmic Microwave Background (CMB); cosmological parameters; hilltop inflation; landscape multiverse; quantum entanglement

1. Introduction

The final Planck likelihood for the data analysis will be released soon. So far, the existence of an intriguing series of anomalies in the CMB has been strongly evidenced by the 2015 Planck collaboration data [1,2] and recently confirmed by the new 2018 data [3,4]. The observed anomalies are consistent with the prediction made in 2005 [5–8], and more recently in [9–11], of the theory of the origin of the universe from the quantum landscape [12–17] multiverse. As we await the final Planck collaboration likelihood release, we complete our investigation of the status of the quantum landscape predictions against data, for a class of concave potential, the hilltop models [18,19].

Hilltop models were investigated in detail in a series of papers in [18,19]. They belong to the class of concave shaped inflationary models, meaning the curvature of their potential $V'' < 0$. These types of potentials are favored by Planck collaboration data [1,4] since they produce a low tensor-to-scalar perturbations ratio r . Corrections to the gravitational potential in the universe, which in the theory of the quantum landscape multiverse, arise from our entanglement with all other structures in the multiverse and give rise to a series of anomalies in the CMB, were derived in [9–11] and analyzed for some concave inflationary models. In this paper, we derive and analyze these corrections against data in the context of Hilltop models.

The paper is organized as follows: in the next Section we present the Hilltop model, and the corrections introduced by the entanglement in the quantum landscape multiverse to the slow-rolling inflaton field and to the inflaton potential, showing as anomalies in the CMB spectrum. In Section 3 we present the method we used for analyzing the model with the data. We provide the results and the likelihood plots in Section 4 for $p = 4$ and Section 5 for $p = 6$. We conclude in Section 6.

2. The Modified Hilltop Potential

The class of Hilltop inflationary models [18,19] describes models where the inflaton starts rolling down from a local maximum. Some of these models are inspired by the F and D-term models of inflation and others by supergravity. The slow roll conditions for the inflaton ϕ are given by $\epsilon = \frac{M_p^2}{2} \left(\frac{V'(\phi)}{V(\phi)} \right)^2 \ll 1$, and, $\eta = M_p^2 \left[\frac{V''(\phi)}{V(\phi)} \right] \ll 1$, where the unmodified potential $V(\phi)$ is of the form:

$$V(\phi) = V_0 \left[1 - \frac{1}{2} c_{hill} \left(\frac{\phi}{M_p} \right)^2 \right] - \lambda_{hill} \left(\frac{\phi^p}{M_p^{p-4}} \right) + \dots \quad (1)$$

and $M_p = 1.2209 \times 10^{19} \text{ GeV}/c^2$ is the Planck mass. Here $c_{hill} = \frac{m^2 M_p^2}{V_0}$, $\lambda_{hill} \ll 1$ are small parameters for slow roll to hold. In this paper, we will focus on $p = 4$ or $p = 6$ models.

From the Friedman equation we have the Hubble expansion parameter

$$3M_p^2 H^2 = V(\phi) \quad (2)$$

Calculating the total number of e-folds N and the power spectrum $P[k]$ from here is well defined and straightforward.

In the presence of corrections, originating from quantum entanglement in the theory of the quantum landscape multiverse, which were derived in [9] for concave potentials [10], the inflaton potential $V(\phi)$ is modified to

$$V_{eff} = V + \frac{1}{2} \frac{V^2}{9M_p^4} F[b, V] = V(\phi) + f[b, V] \quad (3)$$

where $m^2 = \text{Abs}[V'']$, and, $F[b, V(\phi)]$ is the scale dependent correction term from entanglement derived in [9] for concave potentials, with b the landscape parameter indicating the energy scale of the local vacuum.

The energy correction term $f[b, V]$ in the effective potential, Equation (3) is

$$f(\phi) = \frac{1}{2} \left[\frac{V(\phi)}{3M_p^2} \right]^2 F(\phi) \quad (4)$$

The parameter b is a landscape parameter describing SUSY-breaking scale in each vacua, therefore it varies from vacua to vacua. All the entanglement information is contained in $F[b, V]$, which was calculated from entanglement initially [5–8] and then in [9]. It is given by

$$F(\phi) = \frac{3}{2} \left(2 + \frac{m^2 M_p^2}{V(\phi)} \right) \ln \left(\frac{b^2 M_p^2}{V(\phi)} \right) - \frac{1}{2} \left(1 + \frac{m^2}{b^2} \right) e^{-\frac{3b^2 M_p^2}{V(\phi)}} \quad (5)$$

Einstein equations get modified accordingly since the inflaton potential V is now replaced by V_{eff} . This means the Friedmann equation for concave potentials such as the Starobinsky [10] or the Hilltop models, becomes

$$3M_p^2 H^2 = V_{eff} = V + f[b, V] \quad (6)$$

where the correction term in the potential and its higher derivatives satisfy: $f[b, V]/V < 1$, $df/dV < 1$, $d^2 f/dV^2 < 1$, such that the slow roll condition for inflation from V_{eff} holds. (This requirement places a lower bound on the parameter 'b', as shown in [5–8].)

Power spectrum, field solution, tensor, and scalar index, now calculated from the modified potential which includes this correction term V_{eff} , are modified accordingly. The derivative of the effective potential is

$$V'_{eff}(\phi) = V'(\phi)(1 + df(\phi)/dV) \quad (7)$$

where

$$\frac{df}{dV} = \frac{V}{9M_p^4} \left(F[b, V] + \frac{V}{2} dF/dV \right) \quad (8)$$

and

$$\frac{dF}{dV} = - \frac{3 \left(m^2 M_p^2 - M_p^2 (b^2 + m^2) \exp\left[-\frac{3b^2 M_p^2}{V}\right] - 2V - m^2 M_p^2 \ln\left[\frac{b^2 M_p^2}{V}\right] \right)}{2V^2}. \quad (9)$$

The mass of the inflaton field is now obtained from the second derivative of the effective potential

$$V_{eff}''(\phi) = V''(\phi) \left(1 + \frac{df}{dV} \right) + \frac{d^2 f}{dV^2} V'^2. \quad (10)$$

The unmodified field solution for the Hilltop potential is given by integrating

$$\frac{V}{M_p^2 V'} d\phi = -d\ln(k). \quad (11)$$

It gives

$$\frac{\phi_0(k)}{M_p} = \frac{\phi_{i,0}}{M_p} \left(\frac{V_0}{M_p^4} \left(\frac{(k/0.002)^{2c_{hill}}}{\left(x + \frac{4\lambda_{hill}}{c_{hill}} (1 - (k/0.002)^{2c_{hill}})\right)} \right) \right)^{1/(p-2)} \quad (12)$$

where $\phi_{i,0}$ is the initial field value at the onset of slow roll. We take it here to be $\phi_{i,0} = \frac{M_p}{\sqrt{c_{hill}}}$ and $x = \frac{12\lambda_{hill}}{2c_{hill}(1-c_{hill})}$.

In the presence of modifications, the potential is replaced by V_{eff} , therefore the modified field solution obtained by

$$3Hd\phi/dt = -\frac{\partial V_{eff}}{\partial d\phi} \quad (13)$$

satisfies the equation

$$\frac{V_{eff}}{M_p^2 V'_{eff}} d\phi = -d\ln(k) \quad (14)$$

which we integrate to obtain the modified field solution.

Again, in the latter we used $d\phi/dt = Hd\phi/d\ln k$ to have a k -dependent field Equation (13). Please note that the correction term originating from quantum entanglement contained in the complicated expression for $F[b, V(\phi)]$, or accordingly $f[b, V(\phi)]$, is nonlocal and k -dependent. Since it is a derived quantity, not a phenomenological one, its expression leaves no room for tweaking or changing it. Therefore, the series of anomalies induces in the CMB spectrum, we discuss in the next sections below, originating from this term, are also scale dependent and robust predictions (meaning we cannot change them to fit the data).

Since we require that slow roll holds even with correction terms, then we can approximate the integral in Equation (14) as:

$$\int \frac{V_{eff}}{V'_{eff}} d\phi \simeq \left(\frac{1 + f/V}{1 + df/dV} \right) \int \frac{V}{V'}. \quad (15)$$

The Equation (14) gives us the field as a function of k , or equivalently the number of e-folds dN , since it allows us to also integrate dN from start to end of slow roll to get the number of e-folds N_{star} .

For the Hilltop potential of Equation (1), following the above derivation, results in this modified inflaton field solution

$$\frac{\phi(k)}{M_p} = \frac{\tilde{\phi}_i}{M_p} \left(\frac{V_0}{M_p^4} \left(\frac{(k/0.002)^{2\tilde{c}_{hill}}}{\left(\tilde{x} + \frac{4\lambda_{hill}}{\tilde{c}_{hill}} (1 - (k/0.002)^{2\tilde{c}_{hill}})\right)} \right) \right)^{1/(p-2)} \quad (16)$$

Here the fiducial mode is $k = 0.002$ and the “tilde” quantities, are modified quantities of their corresponding unmodified quantities. For example, we have:

$$\tilde{c}_{hill} = c_{hill} \frac{(1 + df/dV)}{(1 + f/V)}, \quad (17)$$

$$\tilde{\eta} = M_p^2 \frac{V''_{eff}}{V_{eff}}, \quad (18)$$

$$\tilde{\epsilon} = \frac{M_p^2 V'_{eff}}{2 V_{eff}}, \quad (19)$$

$$\tilde{\phi}_i = \left(\frac{1}{c_{hill}} \frac{1 + f/V}{1 + df/dV} \right)^{1/(p-2)}, \quad (20)$$

$$\tilde{x} = \frac{12\lambda_{hill}}{2\tilde{c}_{hill}(1 - \tilde{c}_{hill})}. \quad (21)$$

where V_{eff} , V'_{eff} and V''_{eff} are given respectively from Equations (3), (7) and (10). Please note that the correction to the field solution contains $(1 + df/dV)/(1 + f/V)$. Here we demand that \tilde{c}_{hill} , $\tilde{\epsilon}$, $\tilde{\eta}$ continue to satisfy the slow roll conditions, which, as mentioned, allows us to find a lower bound on the parameter b which, in combination with the inflaton potential V , controls the strength of the corrections in V_{eff} .

We can now put everything together to calculate the power spectrum and tensor-to-scalar ratio. The expression below for the power spectrum uses the reduced Planck mass $M = 2.435 \times 10^{18} GeV/c^2$ instead of Planck mass M_p , thus the change in notation from M_p to M (In our analysis all the factors of 2π are carefully taken into account going from M to M_p to ensure consistency.). The modified power spectrum $P_\zeta(k)$, related to its unmodified spectrum $P_0(k)$ is

$$P_\zeta(k) = \frac{1}{24\pi^2 M_p^6} \left[\frac{V_{eff}(\phi)^3}{V'_{eff}(\phi)^2} \right] \simeq P_0[k] \frac{(1 + f/V)^3}{(1 + df/dV)^2} \quad (22)$$

In our notation, unmodified fields and spectra are denoted by $_0$, e.g., ϕ_0, r_0, P_0 and are evaluated with respect to unmodified field. All modified quantities ϕ, r, P etc., denoted without the $_0$, are evaluated with respect to the modified field ϕ , and not ϕ_0 .

The modified tensor-to-scalar ratio is

$$r[k] = 8M_p^2 \left(\frac{V'_{eff}(\phi)}{V_{eff}(\phi)} \right)^2 \quad (23)$$

Using V' and V'_{eff} which we calculated above, we have approximately:

$$r[k] = r_0[k] \left(\frac{1 + df/dV}{1 + f/V} \right)^2. \quad (24)$$

We can also calculate $n[k] - 1 = d \ln(P[k]) / d \ln(k)$ from the expression for $P[k]$ above. Then the unmodified scalar tensor is $n_0[k] - 1 = d \ln(P_0[k]) / d \ln(k)$ where the $_0$ notation means unmodified field and power spectrum and scalar tensor.

With these expressions, we are now ready to check the status of the *modified* Hilltop models against data, for the cases $p = 4$ and $p = 6$: in order to scrutinize the predictions of anomalies from the quantum landscape multiverse; and, check whether the allowed range of the landscape vacuum energy from which our universe inflated, given by the parameter b that controls the corrections in V_{eff} , still satisfies the slow roll conditions.

3. Analysis Method

We will explore the modified Hilltop model by considering the 4 standard cosmological parameters and 4 inflationary parameters. These are, respectively, the baryon energy density $\Omega_b h^2$; the cold dark matter energy density $\Omega_c h^2$; the reionization optical depth τ ; the ratio between the sound horizon and the angular diameter distance at decoupling Θ_s ; the logarithm of the SUSY-breaking scale associated with the landscape effects $\log(b[\text{GeV}])$; the energy scale of the inflation $10^{12} V_0 / M^4$, $10^{11} \lambda_{\text{hill}}$ and c_{hill} .

Furthermore, we will also consider a couple of extensions to this baseline model, by adding one more parameter per time, namely the effective number of relativistic degrees of freedom N_{eff} and the dark energy equation of state w . All the parameters are explored within the range of the conservative flat priors reported in Table 1, for $p = 4$ and $p = 6$.

We show the manner in which the SUSY-breaking scale b affects the CMB temperature, polarization, and matter power spectra, respectively in Figures 1–3: the effect on the power spectra, when increasing the value of b , is an overall decreasing of all the peaks.

Table 1. External priors on the cosmological parameters assumed in this work.

| Parameter | $p = 4$ | $p = 6$ |
|---------------------------------|---------------|---------------|
| $\Omega_b h^2$ | [0.005, 0.1] | [0.005, 0.1] |
| $\Omega_{\text{cdm}} h^2$ | [0.001, 0.99] | [0.001, 0.99] |
| Θ_s | [0.5, 10] | [0.5, 10] |
| τ | [0.01, 0.8] | [0.01, 0.8] |
| $\log(b[\text{GeV}])$ | [1, 19] | [1, 19] |
| $10^{12} V_0 / M^4$ | [0.02, 40] | [10, 80] |
| $10^{11} \lambda_{\text{hill}}$ | [0.2, 0.6] | [0.2, 1.0] |
| c_{hill} | [0, 1] | [0, 0.05] |
| N_{eff} | [0.05, 10] | [0.05, 10] |
| w | [-3.0, 0.3] | [-3.0, 0.3] |

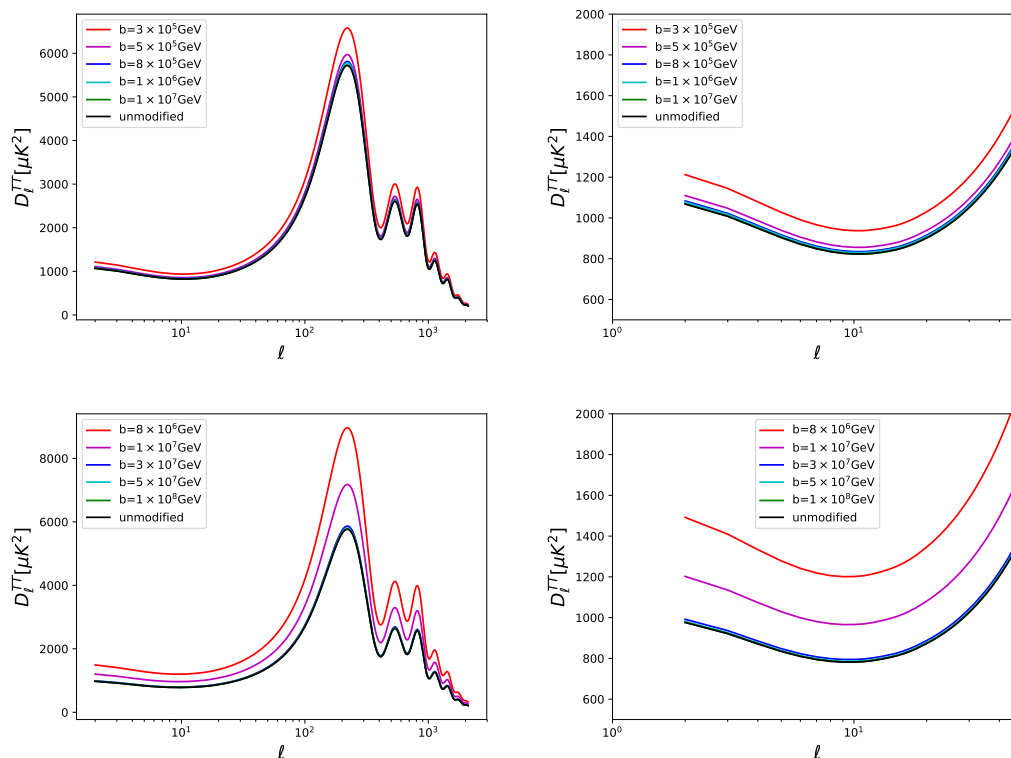


Figure 1. The temperature CMB angular power spectrum by varying the SUSY-breaking scale b associated with the landscape effects, for the modified Hilltop model with $p = 4$ (upper panels) and $p = 6$ (bottom panels).

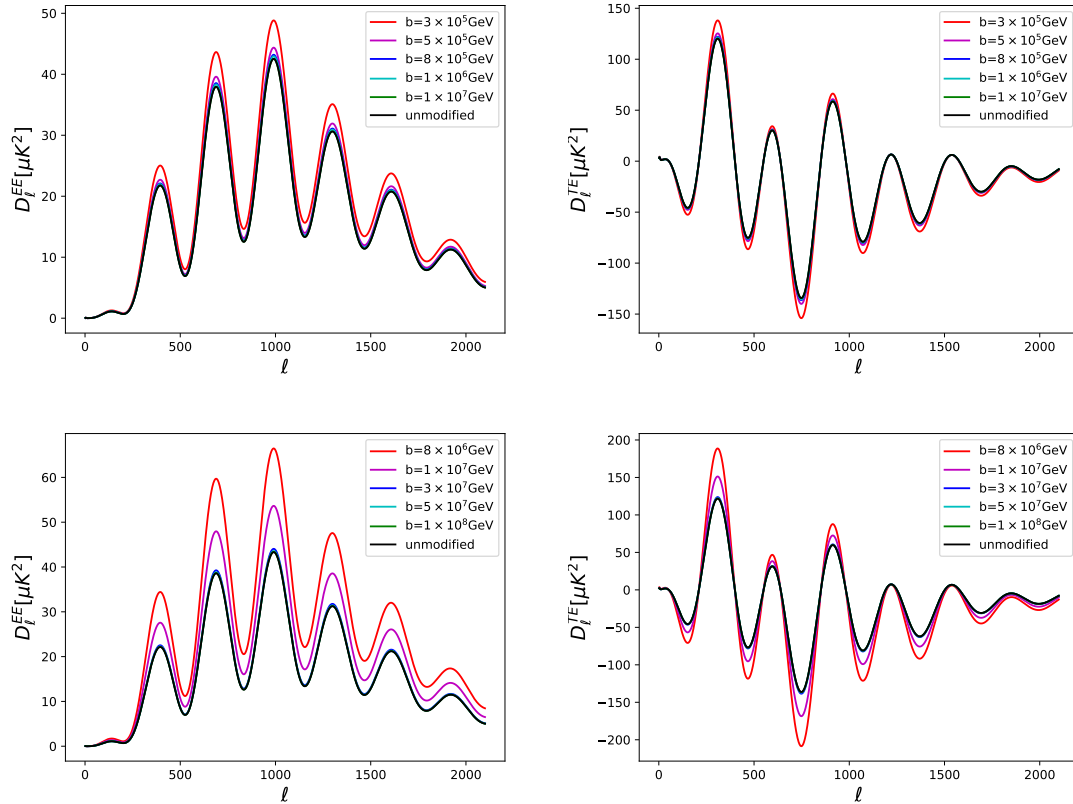


Figure 2. The polarization CMB angular power spectra by varying the SUSY-breaking scale b associated with the landscape effects, for the modified Hilltop model with $p = 4$ (**upper panels**) and $p = 6$ (**bottom panels**).

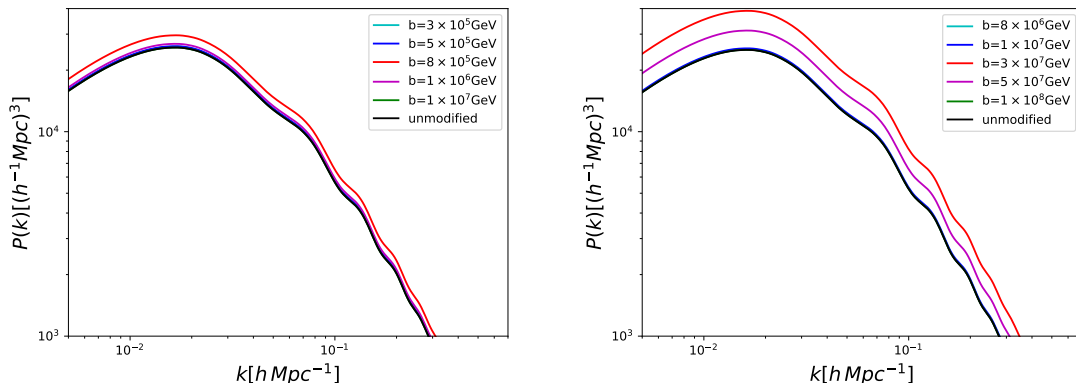


Figure 3. The matter power spectrum by varying the SUSY-breaking scale b associated with the landscape effects, for the modified Hilltop model with $p = 4$ (**left panel**) and $p = 6$ (**right panel**).

We constrained the parameters listed before by considering the following cosmological probes. Firstly, we analyzed the “Planck TT + lowP” data, i.e., the full range of the 2015 temperature power spectrum ($2 \leq \ell \leq 2500$) combined with the low- ℓ polarization power spectra in the multipoles range $2 \leq \ell \leq 29$ provided by the Planck collaboration [20]. Secondly, we included the high multipoles Planck polarization data [20], in the range $30 \leq \ell \leq 2500$, and we called this combination “Planck TTTEEE + lowP”. Then, we replaced the low- ℓ data in the multipoles range $2 \leq \ell \leq 29$ with a gaussian prior on the reionization optical depth $\tau = 0.055 \pm 0.009$, as obtained from Planck HFI measurements [21], and we called this prior “tau055”. Finally, we added the baryon acoustic oscillation data from 6dFGS [22],

SDSS-MGS [23], BOSSLOWZ [24] and CMASS-DR11 [24] surveys as was done in [25], and we referred to this dataset as “BAO”.

To analyze statistically these data exploring the modified Hilltop model for the entanglement, we have used the publicly available Monte-Carlo Markov Chain package cosmomc [26], with a convergence diagnostic based on the Gelman and Rubin statistic, where we modified the CAMB code [27], to include the primordial power spectrum of our model. It implements an efficient sampling of the posterior distribution using the fast/slow parameter decorrelations [28], and it includes the support for the Planck data release 2015 Likelihood Code [20] (see <http://cosmologist.info/cosmomc/>).

4. Results $p = 4$

The result of all the explorations are given in Tables 2–4, where we report the constraints at 95% c.l. on the cosmological parameters. All the bounds that we will quote hereinafter there will be at 95% c.l., unless otherwise expressed. These tables differ for the cosmological scenario explored, respectively the Λ CDM+r, Λ CDM+r+ N_{eff} , w CDM+r. In Table A2 we can see instead the bounds for the same cases for the unmodified Hilltop scenario with $p = 4$.

Table 2. 95% c.l. constraints on cosmological parameters in our baseline Λ CDM+r scenario from different combinations of datasets with a modified Hilltop inflation with $p = 4$.

| Planck TT | Best Fit | | Best Fit | | Best Fit | |
|---------------------------------|---------------------------------|---------|---------------------------------|--------------|---------------------------------|----------|
| | + lowP | + lowP | + lowP + BAO | + lowP + BAO | + tau055 | + tau055 |
| $\Omega_b h^2$ | $0.02225^{+0.00047}_{-0.00044}$ | 0.02225 | $0.02227^{+0.00040}_{-0.00039}$ | 0.02224 | $0.02210^{+0.00042}_{-0.00044}$ | 0.02193 |
| $\Omega_c h^2$ | $0.1195^{+0.0044}_{-0.0042}$ | 0.1199 | $0.1189^{+0.0025}_{-0.0026}$ | 0.1195 | $0.1213^{+0.0044}_{-0.0042}$ | 0.1228 |
| τ | $0.078^{+0.037}_{-0.037}$ | 0.076 | $0.080^{+0.036}_{-0.034}$ | 0.084 | $0.059^{+0.017}_{-0.018}$ | 0.059 |
| $10^{12} V_0 / M^4$ | < 11.7 | 0.70 | < 12.5 | 0.53 | < 29.2 | 5.6 |
| $\log(b[\text{GeV}])$ | > 6.75 | 11.8 | > 6.86 | 13.3 | > 7.44 | 10.2 |
| $10^{11} \lambda_{\text{hill}}$ | $0.304^{+0.059}_{-0.048}$ | 0.276 | $0.304^{+0.063}_{-0.048}$ | 0.280 | $0.36^{+0.12}_{-0.10}$ | 0.31 |
| c_{hill} | 0.0031 ± 0.0012 | 0.0033 | $0.00295^{+0.00094}_{-0.00089}$ | 0.0034 | $0.0033^{+0.0013}_{-0.0012}$ | 0.0037 |
| r | < 0.0941 | 0.0061 | < 0.101 | 0.0046 | < 0.219 | 0.047 |
| H_0 | 67.4 ± 1.9 | 67.2 | $67.7^{+1.2}_{-1.1}$ | 67.5 | $66.6^{+1.8}_{-1.8}$ | 66.0 |
| σ_8 | $0.829^{+0.029}_{-0.028}$ | 0.830 | $0.828^{+0.029}_{-0.028}$ | 0.836 | $0.820^{+0.021}_{-0.020}$ | 0.826 |
| χ^2 | | 11266.6 | | 11271.1 | | 771.4 |
| Planck TTTEEE | Best Fit | | Best Fit | | Best Fit | |
| | + lowP | + lowP | + lowP + BAO | + lowP + BAO | + tau055 | + tau055 |
| $\Omega_b h^2$ | $0.02224^{+0.00032}_{-0.00032}$ | 0.02227 | $0.02228^{+0.00028}_{-0.00026}$ | 0.02234 | $0.02216^{+0.00030}_{-0.00028}$ | 0.02226 |
| $\Omega_c h^2$ | $0.1198^{+0.0028}_{-0.0030}$ | 0.1193 | $0.1192^{+0.0021}_{-0.0021}$ | 0.1181 | 0.1208 ± 0.0027 | 0.1205 |
| τ | $0.078^{+0.034}_{-0.033}$ | 0.091 | $0.082^{+0.032}_{-0.032}$ | 0.091 | $0.061^{+0.017}_{-0.016}$ | 0.073 |
| $10^{12} V_0 / M^4$ | < 13.4 | 0.18 | < 12.4 | 0.17 | < 26.6 | 11.6 |
| $\log(b[\text{GeV}])$ | > 6.90 | 15.7 | > 6.80 | 14.8 | > 7.24 | 16.8 |
| $10^{11} \lambda_{\text{hill}}$ | $0.310^{+0.068}_{-0.049}$ | 0.279 | $0.307^{+0.063}_{-0.047}$ | 0.274 | $0.35^{+0.11}_{-0.09}$ | 0.362 |
| c_{hill} | $0.00318^{+0.00094}_{-0.00099}$ | 0.0033 | $0.00306^{+0.00085}_{-0.00079}$ | 0.0030 | 0.0033 ± 0.0011 | 0.0033 |
| r | < 0.106 | 0.0016 | < 0.0983 | 0.0014 | < 0.199 | 0.091 |
| H_0 | $67.3^{+1.4}_{-1.2}$ | 67.4 | $67.54^{+0.93}_{-0.94}$ | 68.0 | 66.8 ± 1.2 | 67.1 |
| σ_8 | $0.830^{+0.026}_{-0.025}$ | 0.839 | 0.831 ± 0.026 | 0.833 | $0.820^{+0.016}_{-0.015}$ | 0.827 |
| χ^2 | | 12943.7 | | 12949.1 | | 2451.7 |

If we compare Table 2, where there are the constraints for this modified Hilltop inflation with $p = 4$, and the first 2 columns of Table A1, where they are the constraints in the standard Λ CDM+r scenario, we have very robust constraints for all the cosmological parameters with no significant departure from their values with respect to the standard case. Moreover, these bounds are also perfectly consistent with the same cases for the original Hilltop model with $p = 4$, how can be seen by looking at Table A2. However, for our modified Hilltop inflation the χ^2 gets worse, even if with more degrees of freedom.

Regarding the inflationary parameters that describe the theory analyzed here, we have an upper limit of the tensor-to-scalar ratio r , consistent with the Λ CDM+r value. We find for this model and

Planck TT + lowP that $r < 0.0941$ c.l.. If we look at Figure 4, which shows the constraints at 68% and 95% confidence levels on the $10^{12}V_0/M^4$ vs. $\log(b)$ plane, we can see that there exists a lower limit for $b > 5.6 \times 10^6 \text{ GeV}$ and $V_0 < 11.7 \times 10^{-12} M_p^4$ for Planck TT+lowP.

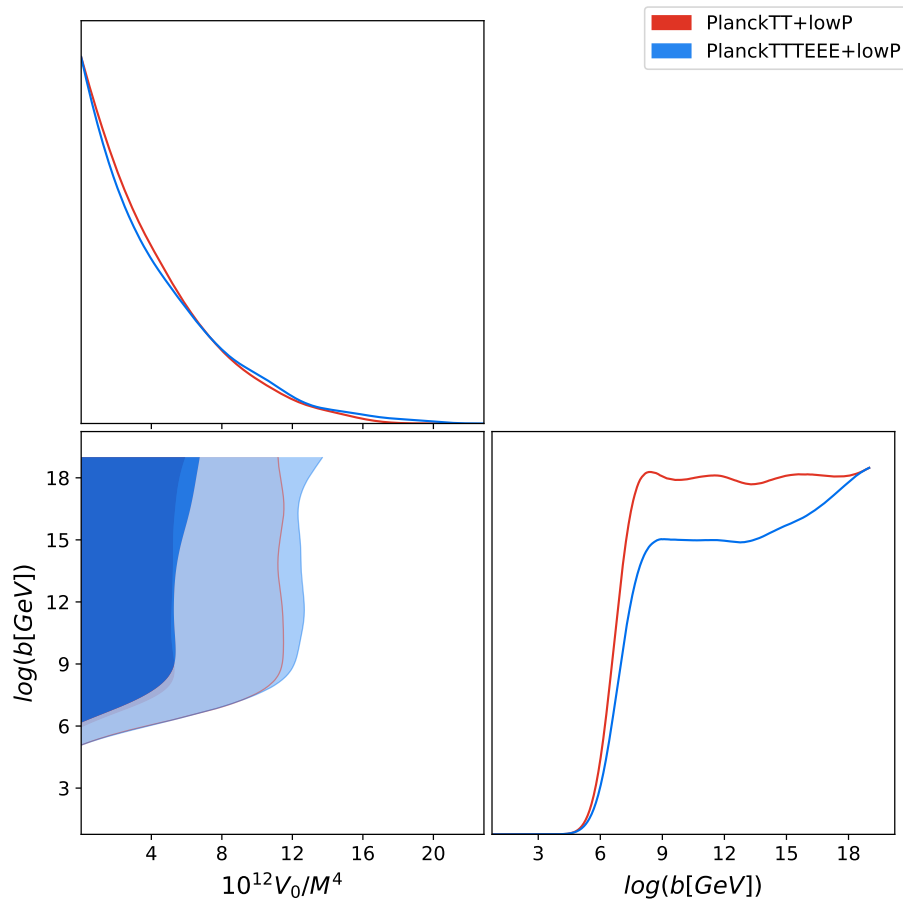


Figure 4. Constraints at 68% and 95% confidence levels on the $10^{12}V_0/M^4$ vs. $\log(b[\text{GeV}])$ plane, in our modified $\Lambda\text{CDM}+r$ Hilltop inflation with $p = 4$. Looking at the Table 2, we can see that the best fits for these parameters are $10^{12}V_0/M^4 = 0.70$ and $\log(b[\text{GeV}]) = 11.8$ for PlanckTT+lowP, while they are $10^{12}V_0/M^4 = 0.18$ and $\log(b[\text{GeV}]) = 15.7$ for PlanckTTTEEE+lowP.

Moreover, by introducing a dark radiation component free to vary N_{eff} in this modified Hilltop scenario with $p = 4$, we have very robust constraints for all the cosmological parameters, see Table 3, which have no significant shifts with respect to the standard $\Lambda\text{CDM}+N_{\text{eff}}$ model (see the columns 3 and 4 of Table A1), and with respect to the original Hilltop model with $p = 4$ (see Table A2). However, also in this case, for our modified Hilltop inflation the χ^2 gets worse. The reason we are introducing this extra parameter is that in the minimal standard cosmological model or in other inflationary models (for example [29,30]), to let N_{eff} free to vary produces a value for this neutrino effective number higher than its expected value 3.045 [31,32], and the shift of the parameters correlated [30,33–36]. In particular, it is interesting to note the shift towards higher values of the Hubble constant H_0 (see Figure 5) that could help in solving the tension now at 3.8σ between the constraints coming from the Planck satellite [3,25,37] and the local measurements of the Hubble constant of Riess et al. [38–40]. In the modified Hilltop scenario, we find the same effect when just the PlanckTT+lowP is considered, and the tension on the Hubble constant becomes of 1.6σ . When introducing the polarization data, the tension with Planck is restored at 2.6σ .

Table 3. 95% c.l. constraints on cosmological parameters in our baseline Λ CDM+r+ N_{eff} scenario from different combinations of datasets with a modified Hilltop inflation with $p = 4$.

| Planck TT | Best Fit | Best Fit | Best Fit | Best Fit | Best Fit |
|---------------------------------|---------------------------------|----------|---------------------------------|--------------|---------------------------------|
| | + lowP | + lowP | + lowP + BAO | + lowP + BAO | + tau055 |
| $\Omega_b h^2$ | $0.02236^{+0.00065}_{-0.00067}$ | 0.02204 | $0.02236^{+0.00048}_{-0.00047}$ | 0.02221 | $0.02183^{+0.00069}_{-0.00072}$ |
| $\Omega_c h^2$ | $0.1210^{+0.0075}_{-0.0077}$ | 0.1203 | $0.1210^{+0.0075}_{-0.0075}$ | 0.1191 | $0.1178^{+0.0077}_{-0.0078}$ |
| τ | $0.082^{+0.041}_{-0.042}$ | 0.078 | $0.082^{+0.035}_{-0.036}$ | 0.075 | $0.058^{+0.017}_{-0.018}$ |
| $10^{12} V_0 / M^4$ | < 11.7 | 0.49 | < 11.7 | 1.8 | < 27.1 |
| $\log(b[\text{GeV}])$ | > 6.42 | 15.3 | > 6.42 | 18.2 | > 7.11 |
| $10^{11} \lambda_{\text{hill}}$ | $0.302^{+0.061}_{-0.047}$ | 0.278 | $0.302^{+0.063}_{-0.049}$ | 0.288 | $0.35^{+0.12}_{-0.09}$ |
| c_{hill} | < 0.00482 | 0.0036 | $0.0025^{+0.0016}_{-0.0017}$ | 0.0036 | $0.0046^{+0.0032}_{-0.0031}$ |
| r | < 0.0928 | 0.016 | < 0.0941 | 0.0013 | < 0.197 |
| N_{eff} | $3.18^{+0.58}_{-0.57}$ | 3.00 | $3.18^{+0.47}_{-0.44}$ | 3.19 | $2.74^{+0.64}_{-0.60}$ |
| H_0 | $68.5^{+5.0}_{-4.9}$ | 66.9 | $68.5^{+3.0}_{-2.9}$ | 68.3 | $64.1^{+5.5}_{-5.4}$ |
| σ_8 | $0.836^{+0.042}_{-0.042}$ | 0.826 | $0.836^{+0.040}_{-0.038}$ | 0.839 | $0.809^{+0.026}_{-0.026}$ |
| χ^2 | | 11268.0 | | 11271.7 | 770.4 |

| Planck TTTEEE | Best Fit | Best Fit | Best Fit | Best Fit | Best Fit |
|---------------------------------|---------------------------------|----------|---------------------------------|--------------|---------------------------------|
| | + lowP | + lowP | + lowP + BAO | + lowP + BAO | + tau055 |
| $\Omega_b h^2$ | $0.02219^{+0.00049}_{-0.00046}$ | 0.02216 | $0.02230^{+0.00038}_{-0.00037}$ | 0.02238 | $0.02195^{+0.00045}_{-0.00046}$ |
| $\Omega_c h^2$ | $0.1192^{+0.0062}_{-0.0059}$ | 0.1194 | $0.1196^{+0.0061}_{-0.0061}$ | 0.1189 | $0.1177^{+0.0063}_{-0.0060}$ |
| τ | 0.077 ± 0.035 | 0.067 | $0.082^{+0.030}_{-0.031}$ | 0.087 | 0.059 ± 0.017 |
| $10^{12} V_0 / M^4$ | < 10.5 | 0.25 | < 12.0 | 1.5 | < 24.4 |
| $\log(b[\text{GeV}])$ | > 6.85 | 8.4 | > 6.77 | 9.0 | > 7.27 |
| $10^{11} \lambda_{\text{hill}}$ | $0.303^{+0.055}_{-0.044}$ | 0.269 | $0.306^{+0.061}_{-0.047}$ | 0.288 | $0.34^{+0.11}_{-0.08}$ |
| c_{hill} | $0.0035^{+0.0018}_{-0.0018}$ | 0.0035 | $0.0030^{+0.0015}_{-0.0014}$ | 0.0033 | $0.0042^{+0.0020}_{-0.0019}$ |
| r | < 0.0841 | 0.0022 | < 0.0957 | 0.013 | < 0.182 |
| N_{eff} | $2.99^{+0.41}_{-0.39}$ | 3.01 | $3.07^{+0.37}_{-0.36}$ | 3.02 | $2.81^{+0.42}_{-0.38}$ |
| H_0 | $66.9^{+3.2}_{-3.0}$ | 66.9 | 67.7 ± 2.4 | 67.4 | $65.1^{+3.2}_{-3.0}$ |
| σ_8 | $0.827^{+0.036}_{-0.034}$ | 0.822 | 0.832 ± 0.032 | 0.834 | 0.810 ± 0.024 |
| χ^2 | | 12946.0 | | 12948.3 | 2447.9 |

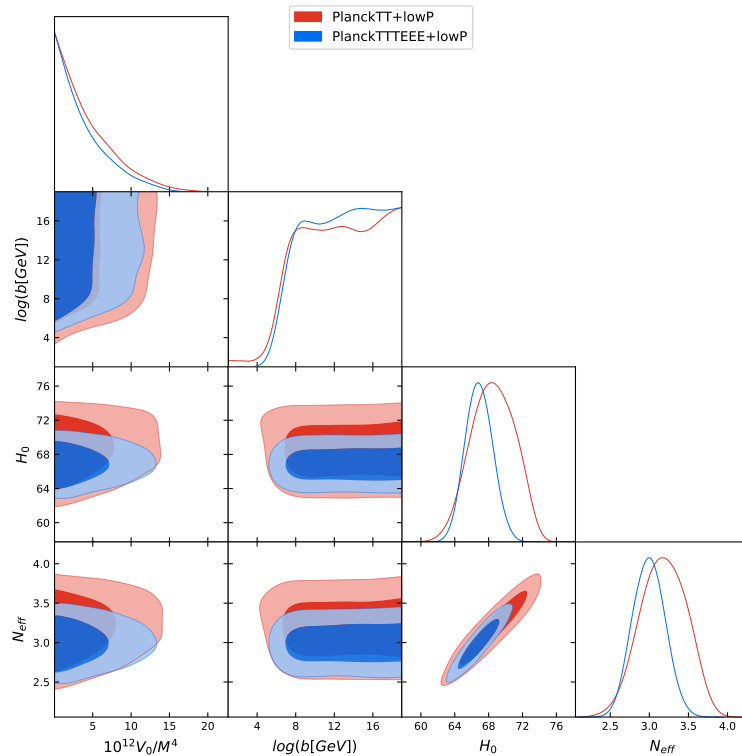


Figure 5. Constraints at 68% and 95% confidence levels in our modified Λ CDM+r+ N_{eff} Hilltop scenario with $p = 4$. Looking at the Table 3, we can see that the best fits for these parameters are $12^{10} V_0 / M^4 = 0.49$, $\log(b[\text{GeV}]) = 15.3$, $N_{\text{eff}} = 3.00$ and $H_0 = 66.9$ for PlanckTT+lowP, while they are $12^{10} V_0 / M^4 = 0.25$, $\log(b[\text{GeV}]) = 8.4$, $N_{\text{eff}} = 3.01$ and $H_0 = 66.9$ for PlanckTTTEEE+lowP.

Regarding the inflationary parameters in this extended Λ CDM+r+ N_{eff} scenario, we still predict a tensor-to-scalar ratio consistent with zero, i.e., $r < 0.0928$ for Planck TT+lowP. Moreover, b still has a lower limit, i.e., $b > 2.6 \times 10^6 \text{ GeV}$ and $V_0 < 11.7 \times 10^{-12} M_p^4$, for Planck TT+lowP datasets.

Finally, in Table 4 we show the constraints for the w CDM+r scenario, using the Hilltop inflationary model with $p = 4$, to test the modifications derived from quantum entanglement from this theory of the origin of the universe. In our modified Hilltop inflationary model, also by varying the equation of state of the dark energy, we find robust constraints for most of the cosmological parameters, which have no significant differences with respect to the standard w CDM model, as shown in the last two columns of Table A1, and with respect to the original Hilltop model with $p = 4$, how can be seen by looking at Table A2. However, also considering these extensions of the model, for our modified Hilltop inflation the χ^2 gets worse. Also, in this case, the mainly reason for extending the baseline scenario is trying to solve the Hubble constant tension, adding a free dark energy equation of state. In fact, the geometrical degeneracy existing between w and H_0 that produces a very large shift of the Hubble constant, unconstrained in this scenario, is very well known. Also, in this modified Hilltop inflation with $p = 4$, as it has been shown by several authors [41–47], the tension is solved with an equation of state $w < -1$. In fact, we have with Planck TTTEEE+lowP $w = -1.56^{+0.59}_{-0.47}$ and $H_0 > 66 \text{ Km/s/Mpc}$, in complete agreement with [39]. However, when we add the BAO dataset, we break their degeneracy and the dark energy equation of state recover the expected value $w = -1$, so a slightly tension at about 2σ reappears in the Hubble constant estimation.

Table 4. 95% c.l. constraints on cosmological parameters in our baseline w CDM+r scenario from different combinations of datasets with a modified Hilltop inflation with $p = 4$.

| Planck TT | Best Fit | | Best Fit | | Best Fit | |
|---------------------------------|---------------------------------|---------|---------------------------------|--------------|---------------------------------|----------|
| | + lowP | + lowP | + lowP + BAO | + lowP + BAO | + tau055 | + tau055 |
| $\Omega_b h^2$ | $0.02228^{+0.00048}_{-0.00044}$ | 0.02236 | $0.02225^{+0.00043}_{-0.00041}$ | 0.02249 | 0.02215 ± 0.00042 | 0.02222 |
| $\Omega_c h^2$ | $0.1193^{+0.0043}_{-0.0045}$ | 0.1193 | 0.1192 ± 0.0038 | 0.1176 | $0.1210^{+0.0041}_{-0.0042}$ | 0.1211 |
| τ | $0.076^{+0.039}_{-0.037}$ | 0.086 | $0.078^{+0.037}_{-0.037}$ | 0.078 | $0.058^{+0.017}_{-0.016}$ | 0.054 |
| $10^{12} V_0 / M^4$ | < 12.5 | 1.6 | < 12.0 | 3.8 | < 28.3 | 1.2 |
| $\log(b[\text{GeV}])$ | > 6.91 | 7.4 | > 6.70 | 17.0 | > 7.12 | 14.4 |
| $10^{11} \lambda_{\text{hill}}$ | $0.306^{+0.063}_{-0.050}$ | 0.284 | $0.303^{+0.062}_{-0.049}$ | 0.294 | $0.35^{+0.12}_{-0.10}$ | 0.273 |
| c_{hill} | $0.0030^{+0.0012}_{-0.0012}$ | 0.0030 | 0.0030 ± 0.0011 | 0.0024 | $0.0032^{+0.0012}_{-0.0012}$ | 0.0038 |
| r | < 0.100 | 0.013 | < 0.0972 | 0.033 | < 0.210 | 0.010 |
| w | $-1.53^{+0.60}_{-0.49}$ | -1.78 | $-1.02^{+0.15}_{-0.15}$ | -0.97 | $-1.48^{+0.69}_{-0.60}$ | -1.68 |
| H_0 | > 65 | 94.1 | $68.1^{+3.4}_{-3.2}$ | 67.3 | > 62 | 88.3 |
| σ_8 | $0.98^{+0.14}_{-0.17}$ | 1.06 | $0.834^{+0.053}_{-0.050}$ | 0.812 | $0.95^{+0.16}_{-0.19}$ | 1.00 |
| χ^2 | | 11262.7 | | 11272.6 | | 769.9 |
| Planck TTTEEE | Best Fit | | Best Fit | | Best Fit | |
| | + lowP | + lowP | + lowP + BAO | + lowP + BAO | + tau055 | + tau055 |
| $\Omega_b h^2$ | $0.02227^{+0.00031}_{-0.00030}$ | 0.02231 | $0.02225^{+0.00030}_{-0.00029}$ | 0.02230 | $0.02218^{+0.00029}_{-0.00028}$ | 0.02231 |
| $\Omega_c h^2$ | $0.1196^{+0.0029}_{-0.0028}$ | 0.1195 | $0.1197^{+0.0029}_{-0.0027}$ | 0.1195 | $0.1206^{+0.0028}_{-0.0028}$ | 0.1201 |
| τ | $0.074^{+0.032}_{-0.034}$ | 0.082 | 0.078 ± 0.033 | 0.090 | $0.060^{+0.017}_{-0.017}$ | 0.055 |
| $10^{12} V_0 / M^4$ | < 13.5 | 0.12 | < 11.9 | 0.62 | < 23.4 | 5.5 |
| $\log(b[\text{GeV}])$ | > 6.96 | 13.5 | > 6.93 | 14.6 | > 7.40 | 14.5 |
| $10^{11} \lambda_{\text{hill}}$ | $0.308^{+0.066}_{-0.051}$ | 0.275 | $0.306^{+0.061}_{-0.048}$ | 0.281 | $0.343^{+0.097}_{-0.087}$ | 0.307 |
| c_{hill} | $0.0031^{+0.0010}_{-0.0009}$ | 0.0034 | $0.00320^{+0.00096}_{-0.00096}$ | 0.0032 | 0.0032 ± 0.0010 | 0.0034 |
| r | < 0.107 | 0.0010 | < 0.0947 | 0.0052 | < 0.178 | 0.046 |
| w | $-1.56^{+0.59}_{-0.47}$ | -1.36 | $-1.03^{+0.11}_{-0.13}$ | -1.04 | $-1.54^{+0.65}_{-0.52}$ | -1.48 |
| H_0 | > 66 | 78.5 | $68.3^{+3.2}_{-2.9}$ | 68.8 | > 64 | 82.4 |
| σ_8 | $0.99^{+0.13}_{-0.17}$ | 0.934 | $0.839^{+0.044}_{-0.040}$ | 0.852 | $0.97^{+0.14}_{-0.18}$ | 0.946 |
| χ^2 | | 12941.8 | | 12950.7 | | 2447.8 |

Regarding the inflationary parameters, again we find just an upper limit for the tensor-to-scalar ratio, i.e., $r < 0.107$, and just a lower limit for the ‘SUSY-breaking’ scale associated with the landscape effects b , i.e., $b > 9.1 \times 10^6 \text{ GeV}$ and $V_0 < 13.5 \times 10^{-12} M_p^4$ for Planck TT+lowP.

If we look at the Figures 6 and 7, we can see the temperature and polarization power spectra obtained with the best fit of our modified Hilltop model with $p = 4$ and the best fit of a minimal

standard cosmological model Λ CDM+r, compared with Planck 2015 TT+lowP data: they are about indistinguishable, fitting the data in the same manner.

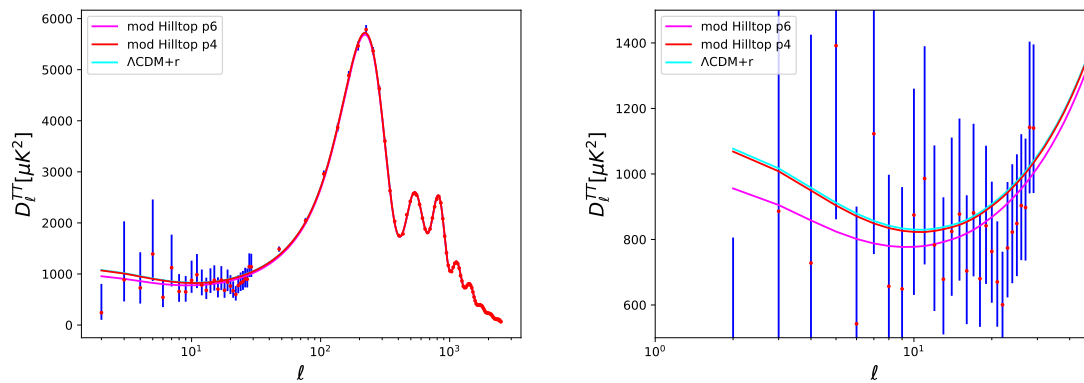


Figure 6. Comparison of the temperature CMB angular power spectrum computed for the best fit of our modified Hilltop model with $p = 6$ (magenta), the best fit of our modified Hilltop model with $p = 4$ (red), and the best fit obtained with a minimal standard cosmological model Λ CDM+r (cyan), with Planck 2015 TT+lowP data (points with error bars). The main differences between the two models are at lower- ℓ and on the amplitude of the peaks that the Hilltop model with $p = 6$, modified for the entanglement, prefers slightly lower.

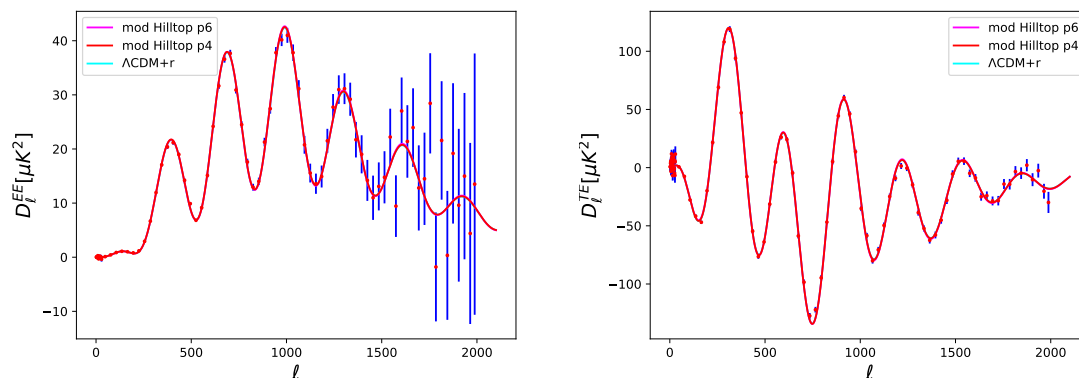


Figure 7. Comparison of the polarization CMB angular power spectra computed for the best fit of our modified Hilltop model with $p = 6$ (magenta), the best fit of our modified Hilltop model with $p = 4$ (red), and the best fit obtained with a minimal standard cosmological model Λ CDM+r (cyan), with Planck 2015 TT+lowP data (points with error bars).

5. Results $p = 6$

The result of all the explorations assuming a modified Hilltop scenario with $p = 6$, are given in Tables 5–7, where we report the constraints at 95% c.l. on the cosmological parameters, respectively for the Λ CDM+r, Λ CDM+r+ N_{eff} , w CDM+r models. In Table A3 we can see instead the bounds for the same cases for the unmodified Hilltop scenario with $p = 6$.

If we compare Table 5, where there are the constraints for this modified Hilltop inflation with $p = 6$, and the constraints obtained in Table 2, where they are those for $p = 4$, we see a very large shift for most of the cosmological parameters. In particular, looking at PlanckTT+lowP we see an important shift of $\Omega_c h^2$, τ and σ_8 at about 2σ towards lower values (see Figure 8), and of H_0 of about 1σ towards a higher one. However, these shifts are not due to our modifications but are characteristic of the Hilltop model with $p = 6$ itself, how can be appreciated by looking at Table A3. In any case, all these shifts are interesting because seem to go in the right direction for solving the several tensions we

see in the cosmological data, between Planck and the other experiments. For example, the well-known degeneracy between the Planck satellite [3,25,37] and the local measurements of the Hubble constant of Riess et al. [38–40], in this case decreased at 2.2σ . Moreover, the tension between Planck and the weak lensing experiments such as the Canada France Hawaii Lensing Survey (CFHTLenS) [48,49], the Kilo Degree Survey of 450 deg² of imaging data (KiDS-450) [50], and the Dark Energy Survey (DES) [51], about the $S_8 \equiv \sigma_8 \sqrt{\Omega_m}/0.3$ value. Thanks to the fact that both the matter density and the clustering parameter are going down in the modified Hilltop model, we find $S_8 = 0.776 \pm 0.027$ at 68% c.l., reducing for example the tension with the value $S_8 = 0.745 \pm 0.039$ at 68% c.l. measured by KiDS-450 [50] within 1σ , as we can see in Figure 9. Finally, the reionization optical depth obtained is now shifted towards lower values, perfectly in agreement with the new $\tau = 0.055 \pm 0.009$ at 68% c.l. obtained from Planck HFI measurements [21] and released in the new Planck 2018 parameters paper [3]. However, for our modified Hilltop inflation the χ^2 gets worse of about 20.

Table 5. 95% c.l. constraints on cosmological parameters in our baseline Λ CDM+r scenario from different combinations of datasets with a modified Hilltop inflation with $p = 6$.

| Planck TT | Best Fit | | Best Fit | | Best Fit | |
|--------------------------|---------------------------------|---------|---------------------------------|--------------|---------------------------------|----------|
| | + lowP | + lowP | + lowP + BAO | + lowP + BAO | + tau055 | + tau055 |
| $\Omega_b h^2$ | $0.02232^{+0.00046}_{-0.00045}$ | 0.02229 | 0.02222 ± 0.00039 | 0.02222 | $0.02222^{+0.00044}_{-0.00043}$ | 0.02209 |
| $\Omega_c h^2$ | $0.1158^{+0.0040}_{-0.0038}$ | 0.1172 | $0.1175^{+0.0024}_{-0.0025}$ | 0.1179 | $0.1181^{+0.0038}_{-0.0036}$ | 0.1191 |
| τ | $0.048^{+0.030}_{-0.031}$ | 0.043 | $0.042^{+0.026}_{-0.029}$ | 0.051 | 0.055 ± 0.017 | 0.057 |
| $10^{12} V_0 / M^4$ | 48 ± 10 | 46 | 49 ± 10 | 48 | 60 ± 10 | 56 |
| $\log(b[GeV])$ | > 8.10 | 11.7 | > 8.01 | 16.8 | > 8.30 | 8.0 |
| $10^{11} \lambda_{hill}$ | > 0.951 | 0.999 | > 0.954 | 0.999 | > 0.936 | 0.998 |
| c_{hill} | $0.00178^{+0.00095}_{-0.00098}$ | 0.0021 | $0.00211^{+0.00070}_{-0.00074}$ | 0.0020 | $0.00234^{+0.00080}_{-0.00083}$ | 0.0025 |
| r | 0.398 ± 0.065 | 0.38 | $0.401^{+0.065}_{-0.064}$ | 0.39 | $0.469^{+0.087}_{-0.077}$ | 0.443 |
| H_0 | 68.9 ± 1.8 | 68.3 | 68.2 ± 1.1 | 68.1 | 67.9 ± 1.7 | 67.4 |
| σ_8 | $0.791^{+0.022}_{-0.023}$ | 0.793 | 0.793 ± 0.021 | 0.800 | $0.806^{+0.016}_{-0.017}$ | 0.810 |
| χ^2 | | 11296.3 | | 11302.4 | | 781.8 |
| Planck TTTEEE | Best Fit | | Best Fit | | Best Fit | |
| | + lowP | + lowP | + lowP + BAO | + lowP + BAO | + tau055 | + tau055 |
| $\Omega_b h^2$ | $0.02226^{+0.00031}_{-0.00032}$ | 0.02213 | $0.02224^{+0.00027}_{-0.00028}$ | 0.02228 | 0.02222 ± 0.00029 | 0.02216 |
| $\Omega_c h^2$ | $0.1179^{+0.0028}_{-0.0027}$ | 0.1183 | $0.1182^{+0.0020}_{-0.0021}$ | 0.1182 | 0.1189 ± 0.0026 | 0.1196 |
| τ | $0.044^{+0.026}_{-0.027}$ | 0.044 | 0.043 ± 0.026 | 0.048 | 0.054 ± 0.016 | 0.054 |
| $10^{12} V_0 / M^4$ | 49 ± 10 | 48 | 50 ± 10 | 50 | 60 ± 10 | 59 |
| $\log(b[GeV])$ | > 8.16 | 18.8 | > 8.24 | 16.5 | > 7.93 | 10.6 |
| $10^{11} \lambda_{hill}$ | > 0.964 | 0.996 | > 0.962 | 0.995 | > 0.957 | 0.999 |
| c_{hill} | $0.00219^{+0.00074}_{-0.00072}$ | 0.0023 | $0.00224^{+0.00065}_{-0.00066}$ | 0.0021 | $0.00249^{+0.00065}_{-0.00066}$ | 0.0027 |
| r | $0.405^{+0.057}_{-0.056}$ | 0.397 | $0.406^{+0.059}_{-0.058}$ | 0.40 | $0.463^{+0.068}_{-0.064}$ | 0.45 |
| H_0 | $68.0^{+1.2}_{-1.3}$ | 67.8 | $67.88^{+0.95}_{-0.91}$ | 67.9 | 67.6 ± 1.2 | 67.3 |
| σ_8 | $0.796^{+0.019}_{-0.020}$ | 0.798 | $0.796^{+0.020}_{-0.019}$ | 0.802 | 0.808 ± 0.015 | 0.811 |
| χ^2 | | 12981.0 | | 12986.4 | | 2466.4 |

Regarding the inflationary parameters that describe the theory analyzed here, we have now a prediction for the tensor-to-scalar ratio r , which in our analysis is a derived parameter, different from zero at many standard deviations. We find for this model and Planck TT + lowP that $r = 0.398 \pm 0.065$, and probably is this value not supported by the data to worsen the χ^2 value. If we look at Figure 10, which shows the constraints at 68% and 95% confidence levels on the $10^{12} V_0 / M^4$ vs. $\log(b)$ plane, we can see that there exists a lower limit for b at $b > 1.3 \times 10^8 GeV$ stronger than the $p = 4$ case and $V_0 = (48 \pm 10) \times 10^{-12} M_p^4$, shifted towards higher values with respect to the $p = 4$ case, for Planck TT+lowP. Finally, we pass from the detection of a value of $\lambda_{hill} = 0.303^{+0.059}_{-0.045}$ in Table 2 to just a lower limit $\lambda_{hill} > 0.951$ in Table 5, and from $c_{hill} = 0.0031 \pm 0.0012$ to $c_{hill} = 0.00178^{+0.00095}_{-0.00098}$ for PlanckTT+lowP.

The same conclusions arise by adding the polarization data of Planck at high- ℓ , the BAO data or by using the “tau055” prior, confirming the robustness of our results.

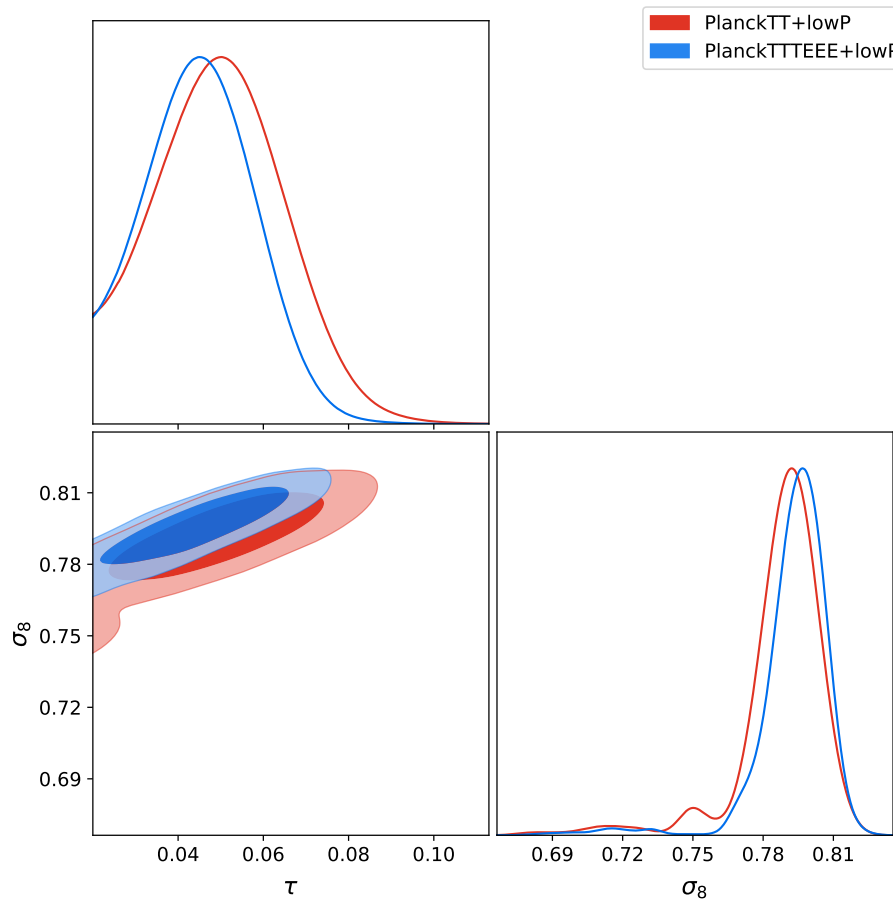


Figure 8. Constraints at 68% and 95% confidence levels on the σ_8 vs. τ plane, in our modified Λ CDM+r Hilltop inflation with $p = 6$. Looking at the Table 5, we can see that the best fits for these parameters are $\sigma_8 = 0.793$ and $\tau = 0.043$ for PlanckTT+lowP, while they are $\sigma_8 = 0.798$ and $\tau = 0.044$ for PlanckTTTEEE+lowP.

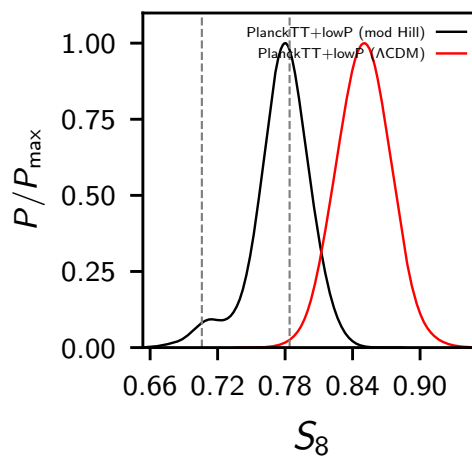


Figure 9. 1D posteriors for our modified Λ CDM+r Hilltop inflation model with $p = 6$ (black solid line) and the standard Λ CDM model (red solid line). The region between the grey dashed lines is the 1σ constraint obtained by KiDS-450.

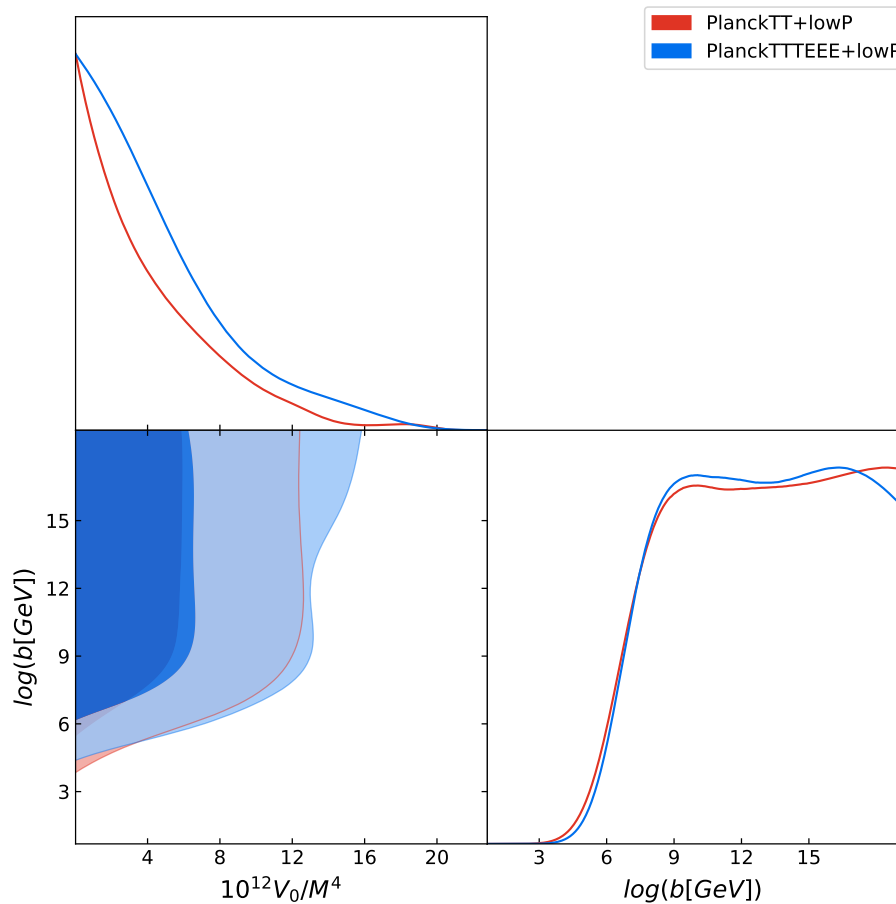


Figure 10. Constraints at 68% and 95% confidence levels on the $10^{12}V_0/M^4$ vs. $\text{Log}(b[\text{GeV}])$ plane, in our modified $\Lambda\text{CDM}+r$ Hilltop inflation with $p = 6$. Looking at the Table 5, we can see that the best fits for these parameters are $10^{12}V_0/M^4 = 46$ and $\text{log}(b[\text{GeV}]) = 11.7$ for PlanckTT+lowP, while they are $10^{12}V_0/M^4 = 48$ and $\text{log}(b[\text{GeV}]) = 18.8$ for PlanckTTTEEE+lowP.

In addition, if we compare Table 6, where there are the constraints for this modified Hilltop scenario with $p = 6$, by introducing a dark radiation component free to vary N_{eff} , and the constraints obtained in the same scenario for $p = 4$ in Table 3, we see a similar shift of the cosmological parameters than in the $\Lambda\text{CDM}+r$ case. However, also in this case these shifts are not related to our modifications but to the Hilltop model with $p = 6$ itself, how can be seen by looking at Table A3. In particular, looking at PlanckTT+lowP we see a shift of $\Omega_c h^2$, τ and σ_8 at about 1σ towards lower values, and of H_0 of more than 1σ towards a higher one, so always in the direction of solving the tensions between the different cosmological probes. In this case, the Hubble constant tension is solved within 1σ , thanks to the evidence for a dark radiation $N_{\text{eff}} > 3.045$ at about 3σ . On the contrary of what usually happens, this evidence is slightly reduced, but not disappears, even when we consider PlanckTTTEEE+lowP, see Figure 11. Therefore, also when the polarization of Planck is added, we can solve the disagreement on the Hubble constant between the CMB and the direct measurements by considering a dark radiation component, as we found also in [11]. Also, in this case the χ^2 value of our modified Hilltop inflation gets worse of about 20 with respect to the standard inflationary model, but it performs about 15 better than the original Hilltop inflation for the Planck TT+lowP case.

Table 6. 95% c.l. constraints on cosmological parameters in our baseline Λ CDM+r+ N_{eff} scenario from different combinations of datasets with a modified Hilltop inflation with $p = 6$.

| Planck TT | Best Fit | | Best Fit | | Best Fit | |
|---------------------------------|---|---------|---|--------------|---|----------|
| | + lowP | + lowP | + lowP + BAO | + lowP + BAO | + tau055 | + tau055 |
| $\Omega_b h^2$ | 0.02236 ^{+0.00041} _{-0.00044} | 0.02278 | 0.02248 ^{+0.00043} _{-0.00044} | 0.02262 | 0.02248 ^{+0.00049} _{-0.00052} | 0.02234 |
| $\Omega_c h^2$ | 0.1236 ^{+0.0068} _{-0.0067} | 0.1245 | 0.1256 ^{+0.0071} _{-0.0073} | 0.1283 | 0.1231 ^{+0.0074} _{-0.0073} | 0.1212 |
| τ | 0.055 ^{+0.026} _{-0.030} | 0.051 | 0.049 ^{+0.028} _{-0.029} | 0.067 | 0.058 ^{+0.016} _{-0.017} | 0.056 |
| $10^{12} V_0 / M^4$ | 46 ± 10 | 40 | 47 ± 10 | 46 | 55 ⁺²⁰ ₋₁₀ | 51 |
| $\log(b[\text{GeV}])$ | > 7.83 | 11.0 | > 7.75 | 9.5 | > 7.55 | 16.8 |
| $10^{11} \lambda_{\text{hill}}$ | > 0.937 | 0.995 | > 0.940 | 0.998 | > 0.916 | 0.993 |
| c_{hill} | < 0.00127 | 0.0000 | < 0.00185 | 0.0000 | < 0.00256 | 0.0017 |
| r | 0.388 ^{+0.068} _{-0.061} | 0.35 | 0.392 ^{+0.071} _{-0.069} | 0.38 | 0.446 ^{+0.097} _{-0.086} | 0.41 |
| N_{eff} | 3.56 ^{+0.30} _{-0.34} | 3.66 | 3.54 ^{+0.36} _{-0.41} | 3.73 | 3.42 ^{+0.44} _{-0.46} | 3.28 |
| H_0 | 72.1 ^{+2.0} _{-2.3} | 73.1 | 71.0 ^{+2.3} _{-2.4} | 72.2 | 70.6 ^{+3.2} _{-3.5} | 69.5 |
| σ_8 | 0.819 ^{+0.027} _{-0.028} | 0.817 | 0.821 ^{+0.032} _{-0.033} | 0.846 | 0.821 ^{+0.026} _{-0.027} | 0.815 |
| χ^2 | | 11287.9 | | 11298.3 | | 781.3 |
| Planck TTTEEE | Best Fit | | Best Fit | | Best Fit | |
| | + lowP | + lowP | + lowP + BAO | + lowP + BAO | + tau055 | + tau055 |
| $\Omega_b h^2$ | 0.02258 ^{+0.00040} _{-0.00042} | 0.02275 | 0.02248 ^{+0.00036} _{-0.00037} | 0.02246 | 0.02236 ± 0.00042 | 0.02216 |
| $\Omega_c h^2$ | 0.1233 ^{+0.0057} _{-0.0058} | 0.1257 | 0.1235 ^{+0.0059} _{-0.0057} | 0.1210 | 0.1213 ^{+0.0061} _{-0.0058} | 0.1180 |
| τ | 0.054 ^{+0.028} _{-0.030} | 0.070 | 0.050 ^{+0.026} _{-0.029} | 0.062 | 0.056 ^{+0.017} _{-0.016} | 0.053 |
| $10^{12} V_0 / M^4$ | 48 ± 10 | 48 | 48 ± 10 | 52 | 58 ± 10 | 56 |
| $\log(b[\text{GeV}])$ | > 7.99 | 18.9 | > 8.02 | 8.4 | > 8.00 | 8.5 |
| $10^{11} \lambda_{\text{hill}}$ | > 0.955 | 0.997 | > 0.956 | 0.994 | > 0.950 | 0.994 |
| c_{hill} | < 0.00212 | 0.0002 | 0.0013 ^{+0.0011} _{-0.0012} | 0.0015 | 0.0020 ^{+0.0012} _{-0.0013} | 0.0026 |
| r | 0.398 ^{+0.063} _{-0.060} | 0.39 | 0.400 ^{+0.058} _{-0.055} | 0.42 | 0.453 ^{+0.076} _{-0.071} | 0.44 |
| N_{eff} | 3.42 ^{+0.33} _{-0.35} | 3.61 | 3.38 ± 0.34 | 3.26 | 3.21 ^{+0.38} _{-0.35} | 3.00 |
| H_0 | 70.6 ^{+2.4} _{-2.6} | 71.8 | 69.9 ^{+2.1} _{-2.2} | 69.4 | 68.7 ^{+2.8} _{-2.6} | 67.4 |
| σ_8 | 0.819 ^{+0.028} _{-0.030} | 83.9 | 0.817 ± 0.030 | 0.819 | 0.816 ^{+0.024} _{-0.023} | 0.803 |
| χ^2 | | 12979.9 | | 12984.3 | | 2466.7 |

Regarding the inflationary parameters also in this Λ CDM+r+ N_{eff} model we have a prediction for the tensor-to-scalar ratio r , which in our analysis is a derived parameter, different from zero: we find for Planck TT + lowP that $r = 0.388^{+0.068}_{-0.061}$, and probably is this value not supported by the data to worsen the χ^2 value. If we look at Figure 11, we can see that there exists a lower limit for $b > 6.8 \times 10^7 \text{ GeV}$ and $V_0 = (46 \pm 10) \times 10^{-12} M_p^4$ for Planck TT+lowP. Finally, also when a dark radiation is included, we pass from the detection of a value of $\lambda_{\text{hill}} = 0.309^{+0.079}_{-0.059}$ in Table 3 to just a lower limit $\lambda_{\text{hill}} > 0.937$ in Table 6, and we obtain a stronger upper bound on $c_{\text{hill}} < 0.00496$ for Λ CDM+r, now $c_{\text{hill}} < 0.00127$ for Λ CDM+r+ N_{eff} , considering PlanckTT+lowP.

When considering PlanckTTTEEE+lowP, the BAO data or the “tau055” prior, we can see that the results are stable, so our conclusions are still valid.

Finally, in Table 7 there are the constraints for the w CDM+r scenario, by varying the equation of state of the dark energy, and using the Hilltop inflationary model with $p = 6$, obtained in our analysis. From the comparison between the Table 7 and the constraints obtained in the same scenario for $p = 4$ in Table 4, we see a similar shift of the cosmological parameters than the previous cases. In particular, looking at PlanckTT+lowP we see a shift of $\Omega_c h^2$ and τ at about 1σ towards lower values, and of H_0 towards a higher one, while σ_8 is stable in this case. Also, in this modified Hilltop inflation with $p = 6$, there is an indication for a dark energy equation of state $w < -1$ at about 3σ , which disappears completely when adding the BAO dataset, restoring the Hubble tension. Again, we can notice that these shifts are not related to our modifications but to the Hilltop model with $p = 6$ itself (Table A3).

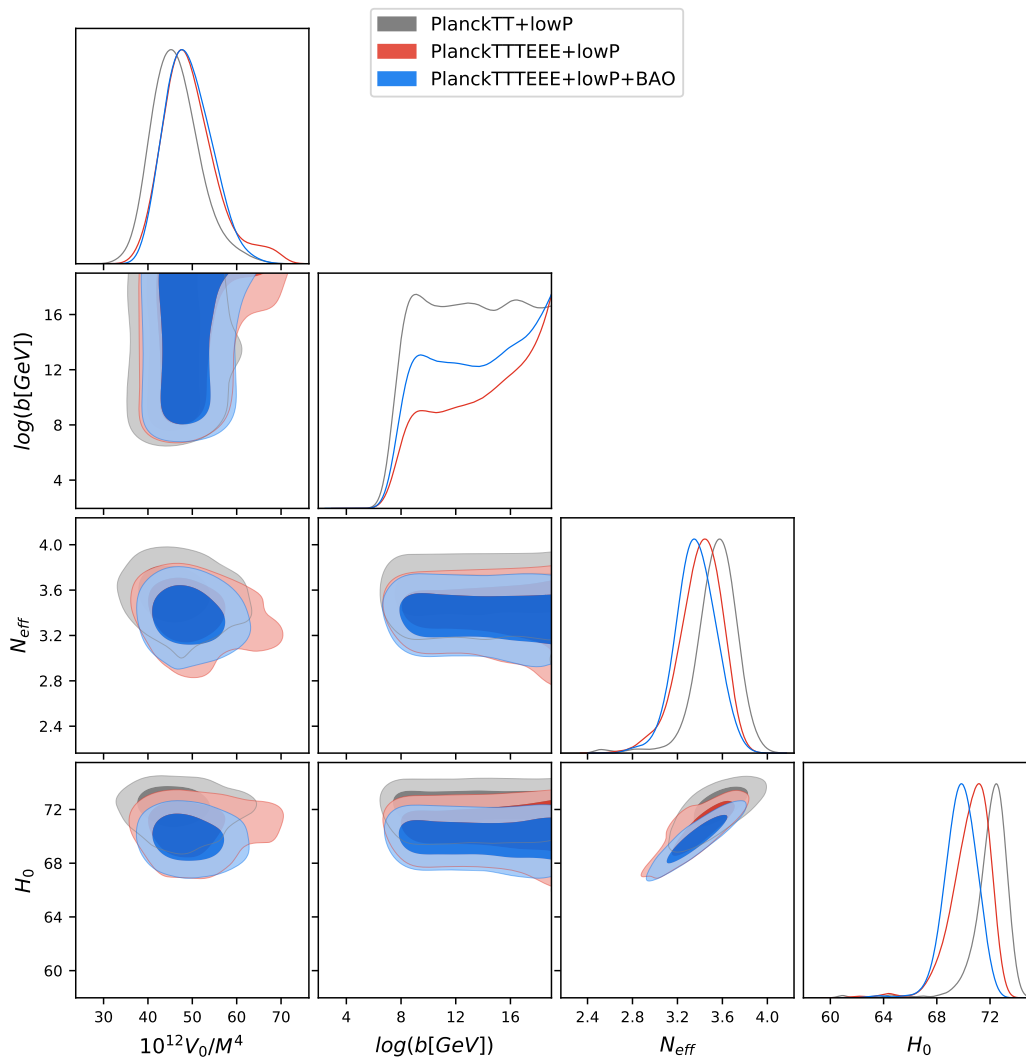


Figure 11. Constraints at 68% and 95% confidence levels in our modified Λ CDM+r+ N_{eff} Hilltop scenario with $p = 6$. Looking at the Table 6, we can see that the best fits for these parameters are $12^{10}V_0/M^4 = 40$, $\log(b[\text{GeV}]) = 11$, $N_{\text{eff}} = 3.66$ and $H_0 = 73.1$ for PlanckTT+lowP, while they are $12^{10}V_0/M^4 = 48$, $\log(b[\text{GeV}]) = 18.9$, $N_{\text{eff}} = 3.61$ and $H_0 = 71.8$ for PlanckTTTEEE+lowP.

Regarding the inflationary parameters, we have still prediction for the tensor-to-scalar ratio r , which in our analysis is a derived parameter, that is $r = 0.400^{+0.064}_{-0.061}$ for PlanckTT+lowP. Probably is this value not supported by the data to worsen the χ^2 value of about 20 if compared with the standard cosmological scenario for the same dataset. Moreover, we find a lower limit for b at $b > 7.1 \times 10^7 \text{ GeV}$, stronger than the $p = 4$ case, and $V_0 = (48 \pm 10) \times 10^{-12} M_p^4$ for Planck TT+lowP. Finally, also when a constant dark energy equation of state is considered, we pass from the detection of a value of $\lambda_{\text{hill}} = 0.311^{+0.088}_{-0.063}$ in Table 4 to just a lower limit $\lambda_{\text{hill}} > 0.947$ in Table 7, and we obtain a stronger bounds on c_{hill} , that is $c_{\text{hill}} = 0.0029^{+0.0013}_{-0.0012}$ for $p = 4$, while becomes $c_{\text{hill}} = 0.00172^{+0.00094}_{-0.00096}$ for $p = 6$, considering PlanckTT+lowP.

When analyzing PlanckTTTEEE+lowP or the “tau055” prior, we can deduce the same conclusions, while the addition of the BAO data changes only our conclusions on w and H_0 as discussed before.

If we look at the Figures 6 and 7, we can see the temperature and polarization power spectra obtained with the best fit of our modified Hilltop model with $p = 6$ and the best fit of a minimal standard cosmological model Λ CDM+r, compared with Planck 2015 TT+lowP data. Our modified Hilltop model fits better the temperature large scales, improving the agreement with the data.

Table 7. 95% c.l. constraints on cosmological parameters in our baseline w CDM+r scenario from different combinations of datasets with a modified Hilltop inflation with $p = 6$.

| Planck TT | Best Fit | | Best Fit | | Best Fit | |
|---------------------------------|---------------------------------|-----------------|---------------------------------|-----------------------|---------------------------------|-------------------|
| | + lowP | + lowP | + lowP + BAO | + lowP + BAO | + tau055 | + tau055 |
| $\Omega_b h^2$ | $0.02239^{+0.00045}_{-0.00044}$ | 0.02246 | 0.02227 ± 0.00042 | 0.02207 | $0.02228^{+0.00043}_{-0.00042}$ | 0.02230 |
| $\Omega_c h^2$ | $0.1156^{+0.0039}_{-0.0038}$ | 0.1148 | 0.1165 ± 0.0035 | 0.1169 | 0.1177 ± 0.0037 | 0.1182 |
| τ | 0.050 ± 0.029 | 0.043 | $0.045^{+0.028}_{-0.031}$ | 0.044 | 0.055 ± 0.017 | 0.052 |
| $10^{12} V_0 / M^4$ | 48 ± 10 | 44 | 48 ± 10 | 46 | 60 ± 10 | 55 |
| $\log(b[\text{GeV}])$ | > 7.85 | 8.6 | > 8.03 | 14.3 | > 8.08 | 11.1 |
| $10^{11} \lambda_{\text{hill}}$ | > 0.947 | 0.988 | > 0.952 | 0.999 | > 0.932 | 0.998 |
| c_{hill} | $0.00172^{+0.00094}_{-0.00096}$ | 0.0016 | $0.00193^{+0.00091}_{-0.00093}$ | 0.0022 | $0.00288^{+0.00079}_{-0.00084}$ | 0.0026 |
| r | $0.400^{+0.064}_{-0.061}$ | 0.38 | $0.398^{+0.065}_{-0.064}$ | 0.39 | $0.466^{+0.087}_{-0.077}$ | 0.43 |
| w | $-1.61^{+0.40}_{-0.31}$ | -1.74 | $-0.96^{+0.12}_{-0.13}$ | -1.00 | $-1.56^{+0.53}_{-0.42}$ | -1.68 |
| H_0 | > 81 | 96.8 | $67.2^{+3.0}_{-2.9}$ | 68.2 | 87^{+10}_{-20} | 91.2 |
| σ_8 | $0.97^{+0.09}_{-0.12}$ | 0.997 | $0.779^{+0.045}_{-0.043}$ | 0.792 | $0.96^{+0.12}_{-0.15}$ | 0.994 |
| χ^2 | | 11289.9 | | 11302.8 | | 778.5 |
| Planck TTTEEE | | | | | | |
| | + lowP | Best Fit + lowP | + lowP + BAO | Best Fit + lowP + BAO | + tau055 | Best Fit + tau055 |
| $\Omega_b h^2$ | $0.02230^{+0.00031}_{-0.00030}$ | 0.02234 | 0.02224 ± 0.00030 | 0.02215 | 0.02226 ± 0.00029 | 0.02234 |
| $\Omega_c h^2$ | 0.1176 ± 0.0027 | 0.1173 | 0.1182 ± 0.0025 | 0.1183 | 0.1186 ± 0.0026 | 0.1184 |
| τ | 0.043 ± 0.027 | 0.43 | 0.043 ± 0.026 | 0.047 | 0.054 ± 0.016 | 0.054 |
| $10^{12} V_0 / M^4$ | 49 ± 10 | 47 | 50^{+10}_{-9} | 49 | 59 ± 10 | 53 |
| $\log(b[\text{GeV}])$ | > 7.95 | 17.3 | > 8.05 | 14.4 | > 7.88 | 11.0 |
| $10^{11} \lambda_{\text{hill}}$ | > 0.960 | 0.991 | > 0.963 | 0.988 | > 0.951 | 0.997 |
| c_{hill} | $0.00215^{+0.00074}_{-0.00078}$ | 0.0022 | $0.00224^{+0.00072}_{-0.00073}$ | 0.0021 | $0.00245^{+0.00064}_{-0.00066}$ | 0.0022 |
| r | $0.403^{+0.061}_{-0.058}$ | 0.39 | $0.407^{+0.057}_{-0.055}$ | 0.40 | $0.460^{+0.070}_{-0.066}$ | 0.42 |
| w | $-1.66^{+0.42}_{-0.32}$ | -1.77 | $-1.01^{+0.11}_{-0.12}$ | -1.05 | $-1.60^{+0.51}_{-0.41}$ | -1.59 |
| H_0 | > 81 | 95.1 | $68.0^{+3.1}_{-2.8}$ | 69.1 | 88^{+10}_{-20} | 87.4 |
| σ_8 | $0.98^{+0.09}_{-0.12}$ | 1.01 | $0.797^{+0.037}_{-0.036}$ | 0.812 | $0.97^{+0.11}_{-0.14}$ | 0.972 |
| χ^2 | | 12973.7 | | 12986.9 | | 2459.9 |

6. Conclusions

The quantum landscape multiverse describes the emergence of the universe from a wavefunction on the landscape before inflation, to a present-day classical universe. Other branches of the wavefunction, originating similarly to ours, are entangled with our universe. This quantum entanglement contributes as a second source a correction term in the gravitational potential of the universe, and it gives rise to modifications of the inflation potential and field evolution.

These modifications, first predicted in [5–8] and then [9] for concave potentials, produce a series of anomalies, such as a suppressed σ_8 , a giant void of size 200 Mpc, suppressed spectrum at low multipoles, and so on. Previously, we checked the status of these predictions with Planck 2015 collaboration data for the exponential and Starobinsky type models of inflation in [10,11]. Here we complete our analysis of the status of the predictions against data with the investigation of a class of concave potential models, the Hilltop potentials.

We ran our analysis for the combined data sets, for the cases $p = 4$ and $p = 6$ of Hilltop models. Both these models allow a range of b where the slow roll regime still holds, and all the predicted anomalies, including the giant void (cold spot) and the suppressed σ_8 , are in very good agreement with data. By considering the quantum entanglement correction of the multiverse, we can place just a lower limit on the local ‘SUSY-breaking’ scale, respectively $b > 8.7 \times 10^6$ GeV at 95% c.l. and $b > 1.3 \times 10^8$ GeV at 95% c.l. from Planck TT+lowP, so the case with multiverse correction is statistically indistinguishable from the case with an unmodified inflation.

Interestingly, the model of $p = 6$ Hilltop inflation, goes beyond the agreement with the datasets for the spectrum and the confirmation of anomalies. This model also reduces the friction between the two major experiments on the value of the Hubble parameter: for $p = 6$ the friction on the Hubble parameter disappears. Moreover, the S_8 values obtained is now perfectly consistent with the weak

lensing experiments. However, this agreement is a characteristic of the Hilltop inflation and not of the modification due to the multiverse.

While we are excited that the anomalies predicted in this theory are in good standing with data independently of the chosen inflationary model, nevertheless we are certainly not claiming that the $p = 6$ Hilltop model including the entanglement corrections from the quantum landscape multiverse, is the only allowed model of inflation. However, it is intriguing and encouraging that such an example where the anomalies are explained and the friction in the Hubble parameter and the S_8 value is removed, without introducing additional ingredients, does exist.

Author Contributions: Conceptualization, E.D.V. and L.M.H.; methodology, E.D.V.; formal analysis, E.D.V.; writing—original draft preparation, E.D.V. and L.M.H.; writing—review and editing, E.D.V. and L.M.H.

Funding: This research was funded by the European Research Council in the form of a Consolidator Grant with number 681431 and the Bahnson funds.

Acknowledgments: EDV acknowledges support from the European Research Council in the form of a Consolidator Grant with number 681431. LMH acknowledges support from the Bahnson funds.

Conflicts of Interest: The authors declare no conflict of interest. The funders had no role in the design of the study; in the collection, analyses, or interpretation of data; in the writing of the manuscript, or in the decision to publish the results.

Appendix A

Table A1. 68% c.l. constraints on cosmological parameters considering the minimal standard cosmological Λ CDM model and its extensions, for different combinations of datasets.

| | Planck TT + lowP | Planck TTTEEE + lowP | Planck TT + lowP | Planck TTTEEE + lowP | Planck TT + lowP | Planck TTTEEE + lowP |
|---------------------|-----------------------|-------------------------|---------------------------|-------------------------|-------------------------|-------------------------|
| $\Omega_b h^2$ | 0.02224 ± 0.00023 | 0.02225 ± 0.00016 | 0.02230 ± 0.00037 | 0.02220 ± 0.00024 | 0.02228 ± 0.00023 | 0.02229 ± 0.00016 |
| $\Omega_c h^2$ | 0.1195 ± 0.0022 | 0.1197 ± 0.0014 | 0.1205 ± 0.0041 | 0.1191 ± 0.0031 | 0.1195 ± 0.0022 | 0.1196 ± 0.0015 |
| τ | 0.077 ± 0.019 | 0.078 ± 0.017 | 0.080 ± 0.022 | 0.077 ± 0.018 | 0.076 ± 0.020 | 0.075 ± 0.017 |
| $\log(10^{10} A_S)$ | 3.087 ± 0.036 | 3.092 ± 0.033 | 3.096 ± 0.047 | 3.088 ± 0.038 | 3.085 ± 0.037 | 3.085 ± 0.033 |
| n_S | 0.9666 ± 0.0062 | 0.9652 ± 0.0047 | 0.969 ± 0.016 | 0.9620 ± 0.0097 | 0.9660 ± 0.0061 | 0.9649 ± 0.0048 |
| r | < 0.0472 | < 0.0463 | (0) | (0) | (0) | (0) |
| N_{eff} | (3.046) | (3.046) | $3.13^{+0.30}_{-0.34}$ | 2.99 ± 0.20 | (3.046) | (3.046) |
| w | (−1) | (−1) | (−1) | (−1) | $-1.54^{+0.20}_{-0.40}$ | $-1.55^{+0.19}_{-0.38}$ |
| H_0 | 67.42 ± 0.99 | 67.31 ± 0.64 | $68.0^{+2.6}_{-3.0}$ | 66.8 ± 1.6 | > 80.9 | > 81.3 |
| σ_8 | 0.828 ± 0.014 | 0.830 ± 0.013 | $0.834^{+0.022}_{-0.025}$ | 0.828 ± 0.018 | $0.98^{+0.11}_{-0.06}$ | $0.98^{+0.10}_{-0.06}$ |
| | Best Fit | Best Fit | Best Fit | Best Fit | Best Fit | Best Fit |
| $\Omega_b h^2$ | 0.02224 | 0.02228 | 0.02224 | 0.02217 | 0.02233 | 0.02230 |
| $\Omega_c h^2$ | 0.1196 | 0.1198 | 0.1196 | 0.1183 | 0.1191 | 0.1195 |
| τ | 0.080 | 0.083 | 0.078 | 0.078 | 0.078 | 0.0747 |
| $\log(10^{10} A_S)$ | 3.093 | 3.101 | 3.089 | 3.087 | 3.088 | 3.082 |
| n_S | 0.9663 | 0.9659 | 0.969 | 0.961 | 0.967 | 0.9654 |
| r | 0.0000 | 0.0001 | (0) | (0) | (0) | (0) |
| N_{eff} | (3.046) | (3.046) | 3.04 | 2.94 | (3.046) | (3.046) |
| w | (−1) | (−1) | (−1) | (−1) | −1.94 | −1.95 |
| H_0 | 67.38 | 67.32 | 67.34 | 66.52 | 100 | 99.9 |
| σ_8 | 0.831 | 0.834 | 0.829 | 0.826 | 1.09 | 1.09 |
| χ^2 | 11261.9 | 12935.6 | 11261.9 | 12935.2 | 11258.9 | 12932.3 |

Table A2. 95% c.l. constraints on cosmological parameters considering the unmodified Hilltop inflationary model with $p = 4$ for different combinations of datasets.

| | Planck TT + lowP | Planck TTTEEE + lowP | Planck TT + lowP | Planck TTTEEE + lowP | Planck TT + lowP | Planck TTTEEE + lowP |
|--------------------------|---------------------------------|---------------------------------|---------------------------------|---------------------------------|------------------------------|---------------------------|
| $\Omega_b h^2$ | $0.02224^{+0.00045}_{-0.00044}$ | $0.02223^{+0.00031}_{-0.00030}$ | $0.02234^{+0.00066}_{-0.00070}$ | $0.02220^{+0.00047}_{-0.00070}$ | 0.02229 ± 0.00045 | 0.02226 ± 0.00031 |
| $\Omega_c h^2$ | $0.1196^{+0.0044}_{-0.0043}$ | 0.1198 ± 0.0029 | $0.1208^{+0.0079}_{-0.0076}$ | $0.1192^{+0.0062}_{-0.0060}$ | $0.1192^{+0.0044}_{-0.0043}$ | 0.1195 ± 0.0029 |
| τ | $0.077^{+0.038}_{-0.037}$ | $0.079^{+0.032}_{-0.33}$ | $0.081^{+0.041}_{-0.039}$ | $0.077^{+0.035}_{-0.034}$ | $0.076^{+0.036}_{-0.037}$ | $0.074^{+0.034}_{-0.033}$ |
| $10^{12} V_0 / M^4$ | < 14.7 | < 13.7 | < 14.5 | < 13.4 | < 14.9 | < 16.8 |
| $10^{11} \lambda_{hill}$ | $0.307^{+0.076}_{-0.055}$ | $0.311^{+0.069}_{-0.050}$ | $0.308^{+0.072}_{-0.052}$ | $0.309^{+0.069}_{-0.051}$ | $0.311^{+0.074}_{-0.056}$ | $0.314^{+0.084}_{-0.059}$ |
| c_{hill} | 0.0031 ± 0.0013 | 0.00318 ± 0.00095 | < 0.00499 | 0.0034 ± 0.0018 | 0.0030 ± 0.0012 | 0.0031 ± 0.0010 |
| r | < 0.116 | < 0.108 | < 0.116 | < 0.105 | < 0.118 | < 0.131 |
| N_{eff} | (3.046) | (3.046) | $3.17^{+0.55}_{-0.59}$ | $3.00^{+0.41}_{-0.39}$ | (3.046) | (3.046) |
| w | (-1) | (-1) | (-1) | (-1) | $-1.54^{+0.59}_{-0.49}$ | $-1.56^{+0.55}_{-0.46}$ |
| H_0 | 67.4 ± 1.9 | 67.3 ± 1.3 | 68.4 ± 5.0 | 66.9 ± 3.1 | > 65 | > 66 |
| σ_8 | 0.828 ± 0.028 | 0.831 ± 0.026 | $0.835^{+0.042}_{-0.041}$ | $0.828^{+0.035}_{-0.034}$ | $0.98^{+0.14}_{-0.17}$ | $0.98^{+0.13}_{-0.16}$ |
| | Best Fit | Best Fit | Best Fit | Best Fit | Best Fit | Best Fit |
| $\Omega_b h^2$ | 0.02216 | 0.02238 | 0.02210 | 0.02224 | 0.02229 | 0.02238 |
| $\Omega_c h^2$ | 0.1222 | 0.1183 | 0.1188 | 0.1175 | 0.1193 | 0.1185 |
| τ | 0.074 | 0.082 | 0.073 | 0.103 | 0.088 | 0.093 |
| $10^{12} V_0 / M^4$ | 0.1 | 0.1 | 2.8 | 0.7 | 3.0 | 15.5 |
| $10^{11} \lambda_{hill}$ | 0.277 | 0.269 | 0.296 | 0.289 | 0.299 | 0.389 |
| c_{hill} | 0.0039 | 0.0030 | 0.0039 | 0.0034 | 0.0030 | 0.0023 |
| r | 0.001 | 0.001 | 0.024 | 0.006 | 0.025 | 0.119 |
| N_{eff} | (3.046) | (3.046) | 2.91 | 3.00 | (3.046) | (3.046) |
| w | (-1) | (-1) | (-1) | (-1) | -0.89 | -1.11 |
| H_0 | 66.3 | 67.9 | 66.0 | 66.9 | 64.3 | 71.4 |
| σ_8 | 0.838 | 0.826 | 0.822 | 0.843 | 0.805 | 0.870 |
| χ^2 | 11264.4 | 12944.8 | 11263.9 | 12943.9 | 11263.7 | 12942.6 |

Table A3. 95% c.l. constraints on cosmological parameters considering the unmodified Hilltop inflationary model with $p = 6$ for different combinations of datasets.

| | Planck TT + lowP | Planck TTTEEE + lowP | Planck TT + lowP | Planck TTTEEE + lowP | Planck TT + lowP | Planck TTTEEE + lowP |
|--------------------------|---------------------------------|---------------------------------|---------------------------------|---------------------------------|---------------------------------|---------------------------------|
| $\Omega_b h^2$ | $0.02233^{+0.00045}_{-0.00044}$ | 0.02226 ± 0.00031 | $0.02264^{+0.00021}_{-0.00044}$ | $0.02258^{+0.00037}_{-0.00041}$ | 0.02239 ± 0.00045 | $0.02230^{+0.00031}_{-0.00030}$ |
| $\Omega_c h^2$ | $0.1158^{+0.0039}_{-0.0038}$ | 0.1179 ± 0.0027 | $0.1234^{+0.0068}_{-0.0065}$ | 0.1232 ± 0.0057 | $0.1156^{+0.0039}_{-0.0038}$ | $0.1176^{+0.0027}_{-0.0028}$ |
| τ | 0.049 ± 0.030 | 0.044 ± 0.027 | $0.055^{+0.026}_{-0.029}$ | $0.055^{+0.027}_{-0.029}$ | 0.049 ± 0.029 | $0.043^{+0.027}_{-0.026}$ |
| $10^{12} V_0 / M^4$ | 48 ± 10 | 50 ± 10 | 46 ± 10 | 48^{+10}_{-9} | 48 ± 10 | 49^{+10}_{-9} |
| $10^{11} \lambda_{hill}$ | > 0.953 | > 0.962 | > 0.941 | > 0.957 | > 0.948 | > 0.961 |
| c_{hill} | $0.00177^{+0.00093}_{-0.00097}$ | $0.00220^{+0.00075}_{-0.00077}$ | < 0.00127 | < 0.00212 | $0.00174^{+0.00091}_{-0.00097}$ | $0.00216^{+0.00075}_{-0.00077}$ |
| r | $0.398^{+0.058}_{-0.057}$ | $0.405^{+0.059}_{-0.056}$ | $0.386^{+0.061}_{-0.057}$ | $0.399^{+0.057}_{-0.055}$ | $0.398^{+0.059}_{-0.057}$ | $0.402^{+0.060}_{-0.055}$ |
| N_{eff} | (3.046) | (3.046) | $3.56^{+0.30}_{-0.32}$ | $3.42^{+0.31}_{-0.35}$ | (3.046) | (3.046) |
| w | (-1) | (-1) | (-1) | (-1) | $-1.61^{+0.40}_{-0.32}$ | $-1.66^{+0.41}_{-0.31}$ |
| H_0 | 69.0 ± 1.8 | $68.0^{+1.3}_{-1.2}$ | $72.1^{+1.9}_{-2.2}$ | $70.6^{+2.3}_{-2.5}$ | > 81 | > 81 |
| σ_8 | $0.792^{+0.022}_{-0.021}$ | 0.796 ± 0.020 | $0.818^{+0.027}_{-0.028}$ | $0.819^{+0.027}_{-0.030}$ | $0.97^{+0.09}_{-0.12}$ | $0.98^{+0.09}_{-0.11}$ |
| | Best Fit |
| $\Omega_b h^2$ | 0.02223 | 0.02223 | 0.02249 | 0.02246 | 0.02236 | 0.02223 |
| $\Omega_c h^2$ | 0.1170 | 0.1179 | 0.1183 | 0.1224 | 0.1151 | 0.1181 |
| τ | 0.041 | 0.034 | 0.031 | 0.041 | 0.024 | 0.033 |
| $10^{12} V_0 / M^4$ | 50 | 54 | 51 | 48 | 52 | 54 |
| $10^{11} \lambda_{hill}$ | 0.965 | 0.933 | 0.880 | 0.957 | 0.885 | 0.938 |
| c_{hill} | 0.0020 | 0.0021 | 0.0007 | 0.0013 | 0.0015 | 0.0022 |
| r | 0.41 | 0.45 | 0.45 | 0.41 | 0.45 | 0.44 |
| N_{eff} | (3.046) | (3.046) | 3.32 | 3.35 | (3.046) | (3.046) |
| w | (-1) | (-1) | (-1) | (-1) | -1.20 | -1.15 |
| H_0 | 68.4 | 68.0 | 71.3 | 69.9 | 75.9 | 72.7 |
| σ_8 | 0.790 | 0.788 | 0.782 | 0.806 | 0.826 | 0.831 |
| χ^2 | 11296.6 | 12979.9 | 11288.7 | 12979.0 | 11288.3 | 12973.5 |

References

1. Ade, P.A.R.; Aghanim, N.; Arnaud, M.; Arroja, F.; Ashdown, M.; Aumont, J.; Baccigalupi, C.; Ballardini, M.; Banday, A.J.; Barreiro, R.B.; et al. Planck 2015 results. XX. Constraints on inflation. *Astron. Astrophys.* **2016**, *594*, A20. [[CrossRef](#)]
2. Ade, P.A.R.; Aghanim, N.; Akrami, Y.; Aluri, P.K.; Arnaud, M.; Ashdown, M.; Aumont, J.; Baccigalupi, C.; Banday, A.J.; Barreiro, R.B.; et al. Planck 2015 results. XVI. Isotropy and statistics of the CMB. *Astron. Astrophys.* **2016**, *594*, A16. [[CrossRef](#)]
3. Aghanim, N.; Akrami, Y.; Ashdown, M.; Aumont, J.; Baccigalupi, C.; Ballardini, M.; Banday, A.J.; Barreiro, R.B.; Bartolo, N.; Basak, S.; et al. Planck 2018 Results. VI. Cosmological Parameters. Available online: <https://arxiv.org/abs/1807.06209> (accessed on 8 April 2019).
4. Akrami, Y.; Arroja, F.; Ashdown, M.; Aumont, J.; Baccigalupi, C.; Ballardini, M.; Banday, A.J.; Barreiro, R.B.; Bartolo, N.; Basak, S.; et al. Planck 2018 Results. X. Constraints on Inflation. Available online: <https://arxiv.org/abs/1807.06211> (accessed on 8 April 2019).
5. Holman, R.; Mersini-Houghton, L.; Takahashi, T. Cosmological avatars of the landscape I: Bracketing the SUSY breaking scale. *Phys. Rev. D* **2008**, *77*, 063510. [[CrossRef](#)]
6. Holman, R.; Mersini-Houghton, L.; Takahashi, T. Cosmological Avatars of the Landscape. II. CMB and LSS Signatures. *Phys. Rev. D* **2008**, *77*, 063511. [[CrossRef](#)]
7. Mersini-Houghton, L. Birth of the Universe from the Multiverse. Available online: <https://arxiv.org/abs/0809.3623> (accessed on 8 April 2019).
8. Mersini-Houghton, L.; Holman, R. 'Tilting' the Universe with the Landscape Multiverse: The 'Dark' Flow. *JCAP* **2009**, *0902*, 006. [[CrossRef](#)]
9. Mersini-Houghton, L. Predictions of the Quantum Landscape Multiverse. *Class. Quant. Grav.* **2017**, *34*, 047001. [[CrossRef](#)]
10. Di Valentino, E.; Mersini-Houghton, L. Testing Predictions of the Quantum Landscape Multiverse 1: The Starobinsky Inflationary Potential. *JCAP* **2017**, *1703*, 002. [[CrossRef](#)]
11. Di Valentino, E.; Mersini-Houghton, L. Testing Predictions of the Quantum Landscape Multiverse 2: The Exponential Inflationary Potential. *JCAP* **2017**, *1703*, 020. [[CrossRef](#)]
12. Mersini-Houghton, L. Can we predict Lambda for the non-SUSY sector of the landscape. *Class. Quant. Grav.* **2005**, *22*, 3481. [[CrossRef](#)]
13. Kobakhidze, A.; Mersini-Houghton, L. Birth of the universe from the landscape of string theory. *Eur. Phys. J. C* **2007**, *49*, 869. [[CrossRef](#)]
14. Mersini-Houghton, L. Wavefunction of the universe on the landscape. *AIP Conf. Proc.* **2006**, *861*, 973. [[CrossRef](#)]
15. Holman, R.; Mersini-Houghton, L. Why the universe started from a low entropy state. *Phys. Rev. D* **2006**, *74*, 123510. [[CrossRef](#)]
16. Holman, R.; Mersini-Houghton, L. Why Did the Universe Start from a Low Entropy State? Available online: <https://arxiv.org/abs/hep-th/0512070> (accessed on 8 April 2019).
17. Mersini-Houghton, L. Cosmological Implications of the String Theory Landscape. *AIP Conf. Proc.* **2006**, *878*, 315. [[CrossRef](#)]
18. Boubekur, L.; Lyth, D.H. Hilltop inflation. *JCAP* **2005**, *0507*, 010. [[CrossRef](#)]
19. Kohri, K.; Lin, C.M.; Lyth, D.H. More hilltop inflation models. *JCAP* **2007**, *0712*, 004. [[CrossRef](#)]
20. Aghanim, N.; Arnaud, M.; Ashdown, M.; Aumont, J.; Baccigalupi, C.; Banday, A.J.; Barreiro, R.B.; Bartlett, J.G.; Bartolo, N.; Battaner, E.; et al. Planck 2015 results. XI. CMB power spectra, likelihoods, and robustness of parameters. *Astron. Astrophys.* **2016**, *594*, A11. [[CrossRef](#)]
21. Aghanim, N.; Ashdown, M.; Aumont, J.; Baccigalupi, C.; Ballardini, M.; Banday, A.J.; Barreiro, R.B.; Bartolo, N.; Basak, S.; Battye, R.; et al. Planck intermediate results. XLVI. Reduction of large-scale systematic effects in HFI polarization maps and estimation of the reionization optical depth. *Astron. Astrophys.* **2016**, *596*, A107. [[CrossRef](#)]
22. Beutler, F.; Blake, C.; Colless, M.; Jones, D.H.; Staveley-Smith, L.; Campbell, L.; Parker, Q.; Saunders, W. The 6dF Galaxy Survey: Baryon Acoustic Oscillations and the Local Hubble Constant. *Mon. Not. Roy. Astron. Soc.* **2011**, *416*, 3017. [[CrossRef](#)]

23. Ross, A.J.; Samushia, L.; Howlett, C.; Percival, W.J.; Burden, A.; Manera, M. The Clustering of the SDSS DR7 Main Galaxy Sample I: A 4 per cent Distance Measure at $z = 0.15$. *Mon. Not. Roy. Astron. Soc.* **2015**, *449*, 835. [[CrossRef](#)]
24. Anderson, L.; Aubourg, É.; Bailey, S.; Beutler, F.; Bhardwaj, V.; Blanton, M.; Bolton, A.S.; Brinkmann, J.; Brownstein, J.R.; Burden, A. et al. The clustering of galaxies in the SDSS-III Baryon Oscillation Spectroscopic Survey: baryon acoustic oscillations in the Data Releases 10 and 11 Galaxy samples. *Mon. Not. Roy. Astron. Soc.* **2014**, *441*, 24. [[CrossRef](#)]
25. Ade, P.A.R.; Aghanim, N.; Arnaud, M.; Ashdown, M.; Aumont, J.; Baccigalupi, C.; Banda, A.J.; Barreiro, R.B.; Bartlett, J.G.; Bartolo, N.; et al. Planck 2015 results. XIII. Cosmological parameters. *Astron. Astrophys.* **2016**, *594*, A13. [[CrossRef](#)]
26. Lewis, A.; Bridle, S. Cosmological parameters from CMB and other data: A Monte Carlo approach. *Phys. Rev. D* **2002**, *66*, 103511. [[CrossRef](#)]
27. Lewis, A.; Challinor, A.; Lasenby, A. Efficient computation of CMB anisotropies in closed FRW models. *Astrophys. J.* **2000**, *538*, 473. [[CrossRef](#)]
28. Lewis, A. Efficient sampling of fast and slow cosmological parameters. *Phys. Rev. D* **2013**, *87*, 103529. [[CrossRef](#)]
29. Tram, T.; Vallance, R.; Vennin, V. Inflation Model Selection meets Dark Radiation. *JCAP* **2017**, *1701*, 046. [[CrossRef](#)]
30. Di Valentino, E.; Bouchet, F.R. A comment on power-law inflation with a dark radiation component. *JCAP* **2016**, *1610*, 011. [[CrossRef](#)]
31. Mangano, G.; Miele, G.; Pastor, S.; Pinto, T.; Pisanti, O.; Serpico, P.D. Relic neutrino decoupling including flavor oscillations. *Nucl. Phys. B* **2005**, *729*, 221. [[CrossRef](#)]
32. De Salas, P.F.; Pastor, S. Relic neutrino decoupling with flavour oscillations revisited. *JCAP* **2016**, *1607*, 051. [[CrossRef](#)]
33. Heavens, A.; Jimenez, R.; Verde, L. Standard rulers, candles, and clocks from the low-redshift Universe. *Phys. Rev. Lett.* **2014**, *113*, 241302. [[CrossRef](#)] [[PubMed](#)]
34. Di Valentino, E.; Giusarma, E.; Mena, O.; Melchiorri, A.; Silk, J. Cosmological limits on neutrino unknowns versus low redshift priors. *Phys. Rev. D* **2016**, *93*, 083527. [[CrossRef](#)]
35. Archidiacono, M.; Giusarma, E.; Hannestad, S.; Mena, O. Cosmic dark radiation and neutrinos. *Adv. High Energy Phys.* **2013**, *2013*, 191047. [[CrossRef](#)]
36. Di Valentino, E.; Boehm, C.; Hivon, E.; Bouchet, F.R. Reducing the H_0 and σ_8 tensions with Dark Matter-neutrino interactions. *Phys. Rev. D* **2018**, *97*, 043513. [[CrossRef](#)]
37. Ade, P.A.R.; Aghanim, N.; Armitage-Caplan, C.; Arnaud, M.; Ashdown, M.; Atrio-Barandela, F.; Aumont, J.; Baccigalupi, C.; Banday, A.J.; Barreiro, R.B.; et al. Planck 2013 results. XVI. Cosmological parameters. *Astron. Astrophys.* **2014**, *571*, A16. [[CrossRef](#)]
38. Riess, A.G.; Macri, L.; Casertano, S.; Lampeitl, H.; Ferguson, H. C.; Filippenko, A.V.; Jha, S.W.; Li, W.; Chornock, R. A 3% Solution: Determination of the Hubble Constant with the Hubble Space Telescope and Wide Field Camera 3. *Astrophys. J.* **2011**, *730*, 119. [[CrossRef](#)]
39. Riess, A.G.; Macri, L. M.; Hoffmann, S.L.; Scolnic, D.; Casertano, S.; Filippenko, A.V.; Tucker, B. E.; Reid, M.J.; Jones, D.O.; Silverman, J. M.; et al. A 2.4 % Determination of the Local Value of the Hubble Constant. *Astrophys. J.* **2016**, *826*, 56. [[CrossRef](#)]
40. Riess, A.G.; Casertano, S.; Yuan, W.; Macri, L.; Bucciarelli, B.; Lattanzi, M.G.; MacKenty, J.W.; Bowers, J.B.; Zheng, W.; Filippenko, A.V.; et al. Milky Way Cepheid Standards for Measuring Cosmic Distances and Application to Gaia DR2: Implications for the Hubble Constant. *Astrophys. J.* **2018**, *861*, 126. [[CrossRef](#)]
41. Di Valentino, E.; Melchiorri, A.; Silk, J. Reconciling Planck with the local value of H_0 in extended parameter space. *Phys. Lett. B* **2016**, *761*, 242. [[CrossRef](#)]
42. Huang, Q.G.; Wang, K. How the dark energy can reconcile Planck with local determination of the Hubble constant. *Eur. Phys. J. C* **2016**, *76*, 506. [[CrossRef](#)]
43. Yang, W.; Pan, S.; Di Valentino, E.; Nunes, R.C.; Vagnozzi, S.; Mota, D.F. Tale of stable interacting dark energy, observational signatures, and the H_0 tension. *JCAP* **2018**, *1809*, 019. [[CrossRef](#)]
44. Di Valentino, E.; Melchiorri, A.; Mena, O. Can interacting dark energy solve the H_0 tension? *Phys. Rev. D* **2017**, *96*, 043503. [[CrossRef](#)]

45. Di Valentino, E.; Melchiorri, A.; Silk, J. Beyond six parameters: Extending Λ CDM. *Phys. Rev. D* **2015**, *92*, 121302. [[CrossRef](#)]
46. Di Valentino, E.; Melchiorri, A.; Linder, E.V.; Silk, J. Constraining Dark Energy Dynamics in Extended Parameter Space. *Phys. Rev. D* **2017**, *96*, 023523. [[CrossRef](#)]
47. Mörtzell, E.; Dhawan, S. Does the Hubble constant tension call for new physics? *JCAP* **2018**, *1809*, 025. [[CrossRef](#)]
48. Heymans, C.; Waerbeke, L.; Miller, L.; Erben, T.; Hildebrandt, H.; Hoekstra, H.; Kitching, T.D.; Mellier, Y.; Simon, P.; Bonnett, C.; et al. CFHTLenS: The Canada-France-Hawaii Telescope Lensing Survey. *Mon. Not. Roy. Astron. Soc.* **2012**, *427*, 146. [[CrossRef](#)]
49. Erben, T.; Hildebrandt, H.; Miller, L.; Waerbeke, L.; Heymans, C.; Hoekstra, H.; Kitching, T.D.; Mellier, Y.; Benjamin, J.; Blake, C.; et al. CFHTLenS: The Canada-France-Hawaii Telescope Lensing Survey - Imaging Data and Catalogue Products. *Mon. Not. Roy. Astron. Soc.* **2013**, *433*, 2545. [[CrossRef](#)]
50. Hildebrandt, H.; Viola, M.; Heymans, C.; Joudaki, S.; Kuijken, K.; Blake, C.; Erben, T.; Joachimi, B.; Klaes, D.; Miller, L.; et al. KiDS-450: Cosmological parameter constraints from tomographic weak gravitational lensing. *Mon. Not. Roy. Astron. Soc.* **2017**, *465*, 1454. [[CrossRef](#)]
51. Abbott, T.M.C.; Abbott, T.M.C.; Abdalla, F.B.; Alarcon, A.; Aleksić, J.; Allam, S.; Allen, S.; Amara, A.; Annis, J.; Asorey, J.; et al. Dark Energy Survey year 1 results: Cosmological constraints from galaxy clustering and weak lensing. *Phys. Rev. D* **2018**, *98*, 043526. [[CrossRef](#)]



© 2019 by the authors. Licensee MDPI, Basel, Switzerland. This article is an open access article distributed under the terms and conditions of the Creative Commons Attribution (CC BY) license (<http://creativecommons.org/licenses/by/4.0/>).